

See discussions, stats, and author profiles for this publication at: <https://www.researchgate.net/publication/317286221>

Design and Fabrication of Hybrid Rocket Motor

Thesis · June 2017

DOI: 10.13140/RG.2.2.36756.50563

CITATIONS

0

READS

331

5 authors, including:



Bilal Siddiqui

Air University of Islamabad

40 PUBLICATIONS 25 CITATIONS

SEE PROFILE

Some of the authors of this publication are also working on these related projects:



Automatic Flight Control Systems [View project](#)



GPS Denied Navigation [View project](#)

Design and Fabrication of Hybrid Rocket Motor

By

Khizar Siddiqui ME-131028

Waqas Aslam ME-131050

Umer Shakeel ME-131045

Syed Mohsin Ali ME-131040

Supervisor: Dr. Bilal A. Siddiqui (ME Dept.)

**A thesis submitted to the Faculty of Mechanical Engineering in
fulfillment of the requirements for the ME-492 Design Project II
course of**

Bachelor of Engineering

In

Mechanical Engineering

DHA Suffa University

Karachi, Pakistan

Table of Contents

Table of Contents.....	i
List of Tables.....	iii
List of Figures.....	iv
Nomenclature.....	viii
Chapter 1: Introduction	1
1.1 Motivation	1
1.2 Objective	2
1.3 Statement of Requirements	2
Chapter 2: Literature Review	7
Chapter 3: Design and Methodology	9
3.1 Fuel Grain Composition	9
3.2 Fuel Testing Engine	12
3.3 Fuel Compositions	13
3.4 Fuel Tests Result	21
3.5 Grain Manufacturing.....	22
3.6 Oxidizer tank	29
3.7 Pipes and Fittings	30
3.8 Igniter	32

3.9	Automating the Design Process and Analysis.....	34
3.10	Calculations	43
3.11	Manufacturing Drawings.....	47
3.12	CAD Drawings	52
3.13	Analysis	55
3.14	Flow Simulation	59
3.15	Test Rigs	61
Chapter 4: Safety		63
Chapter 5: Manufacturing Processes		65
5.1	Combustion Chamber.....	65
5.2	Injector Assembly	66
5.3	Con-Di.....	70
5.4	End cap.....	71
Chapter 6: Results and Conclusion.....		72
6.1	Results and discussion.....	72
6.2	Conclusion.....	79

List of Tables

Table 1: Fuel Composition 2	14
Table 2: Fuel Composition 3	16
Table 3: Fuel Composition 4	17
Table 4: Fuel Composition 5	19
Table 5: Ingredients of black powder	32
Table 6: Description for Code Inputs	34

List of Figures

Figure 3-1 Paraffin Wax	9
Figure 3-2 Microcrystalline Wax.....	10
Figure 3-3 Poly ethylene wax	10
Figure 3-4 Carnauba wax	11
Figure 3-5 Fuel Testing Engine	12
Figure 3-6 Fuel composition 1	13
Figure 3-7 Test on Fuel composition 1	14
Figure 3-8 Fuel composition 2	15
Figure 3-9 Test on Fuel composition 2 a	15
Figure 3-10 Test on Fuel composition 2 b	16
Figure 3-11 Test on Fuel composition 3	17
Figure 3-12 First Test on Fuel composition 4	18
Figure 3-13 Second Test on Fuel composition 4	18
Figure 3-14 Fuel composition 5	19
Figure 3-15 Tests on Fuel composition 5.....	20
Figure 3-16 Regression Rate Comparison	21
Figure 3-17 Irregular Burning	22
Figure 3-18 Non-Homogeneity of Waxes	23
Figure 3-19 Mandrel.....	24
Figure 3-20 Molding Assembly.....	25
Figure 3-21 Left: Mould Pressurization; Right: Wax Overflow	26
Figure 3-22 Chamber Mounted on Lathe Machine	27
Figure 3-23 Chamber Rotating at a constant RPM on Lathe Machine	27
Figure 3-24 Top of the Solidified Mould.....	28
Figure 3-25 Bottom of the Solidified Mould	28

Figure 3-26 Cylinder Assembly	29
Figure 3-27 Attachments	30
Figure 3-28 Pipes Rating	31
Figure 3-29 Ball Valve	31
Figure 3-30 T-Connectors	31
Figure 3-31 Igniter Assembly	33
Figure 3-32 Variation of Combustion Temperature with OFR.....	36
Figure 3-33 Variation in I_{sp} with OFR	36
Figure 3-34 Variations of Flow Properties along Nozzle Axis	38
Figure 3-35 Thermal Model of Combustion Chamber	39
Figure 3-36 Electrical Analogy of Heat Transfer through Combustion Chamber	39
Figure 3-37 Throat data from MATLAB	43
Figure 3-38 Combustion Chamber Data from MATLAB	43
Figure 3-39 Production Drawing of Combustion Chamber.....	47
Figure 3-40 Production Drawing of Injector cap	48
Figure 3-41 Production Drawing of Injector Disc.....	49
Figure 3-42 Production Drawing of Con-Di Nozzle.....	50
Figure 3-43 Production Drawing of End Cap	51
Figure 3-44 Rocket Assembly	52
Figure 3-45 Rocket Assembly Section View	52
Figure 3-46 Con-Di Nozzle	53
Figure 3-47 Con-Di Nozzle Section View	53
Figure 3-48 Injector Assembly	54
Figure 3-49 Rocket Assembly Exploded View.....	54
Figure 3-50: FEA simulations on the Combustion chamber.....	55
Figure 3-51 Injector Disc FEA Simulation (view 1).....	56
Figure 3-52 Injector Disc FEA Simulation (view 2).....	56
Figure 3-53 Injector Cap FEA Simulation (view 1).....	57

Figure 3-54 Injector Cap FEA Simulation (view 2).....	57
Figure 3-55 Assembly FEA Simulation.....	58
Figure 3-56 Velocity Simulation without Fuel Grain	59
Figure 3-57 Mach No. Simulation without Fuel Grain.....	59
Figure 3-58 Velocity Simulation with Fuel Grain	60
Figure 3-59 Mach No. Simulation with Fuel Grain	60
Figure 3-60 Test Rig CAD Drawings	61
Figure 3-61 Test Rig with Rocket Mounted	62
Figure 3-62 Load Cell.....	62
Figure 4-1 Grinding with Safety.....	63
Figure 4-2 Mould Handling with Safety	64
Figure 4-3 Safe Distance.....	64
Figure 5-1 Injector assembly	66
Figure 5-2: Injector assembled in the rocket (pipes are shown too).....	67
Figure 5-3 Injector cap isometric View.....	67
Figure 5-4 Injector cap Top View	68
Figure 5-5 Injector Disc Top View	69
Figure 5-6 Injector Disc Isometric View	69
Figure 5-7 Con-Di Isometric View	70
Figure 5-8 Manufacturing of End Cap	71
Figure 5-9 End Cap Isometric View.....	71
Figure 6-1 Flame Geometry 1.....	72
Figure 6-2 Flame Geometry 2	72
Figure 6-3 MS Plate.....	73
Figure 6-4 Mild Steel Plate with Broken Welds (post test)	73
Figure 6-5 Mild Steel Plate Front View (post test).....	74
Figure 6-6 Test Rig Failure Analysis 1.....	75
Figure 6-7 Test Rig Failure Analysis 2.....	75

Figure 6-8 Test Rig Failure Analysis 3.....	76
Figure 6-9 Test Rig Failure Analysis 4.....	76
Figure 6-10 Test Rig Failure Analysis 5.....	77
Figure 6-11 Manual Deflection Measurement.....	78

Nomenclature

E	Young's Modulus of Elasticity (MPa)
h	Convective heat transfer coefficient (W/m ² K)
A	Area [m ²]
a	Speed of sound [m/s]
C_d	Discharge coefficient
C_p	Specific heat at constant pressure [J/kg.K]
C_v	Specific heat at constant volume [J/kg.K]
D	Diameter [m]
F	Thrust force [N]
g	Gravitational acceleration [m/s ²]
H	Height [m]
h	Specific enthalpy [J/kg]
I_{sp}	Specific impulse [s]
K	Thermal conductivity [W/m.K]
L	Length [m]
M	Molar mass [kg/kmol]
M_a	Mach number
m^*	Mass flow rate [kg/s]
OF	Oxidizer-to-fuel ratio
P	Pressure [Pa]
q	Heat power, heat transfer rate [W]
q''	Heat flux [W/m ²]
R	Universal gas constant (J/kmol.K) [J/kmol.K]

r	Regression rate [m/s]
S	Surface area [m^2]
s	Specific entropy [J/kg.K]
T	Temperature [K]
U	Velocity [m/s]
<i>u</i>	Specific internal energy [J/kg]
V	Volume [m^3]
HTPB	Hydroxyl-Terminated Polybutadiene
CB	Carbon black

ACKNOWLEDGEMENT

We sincerely thank Dr. Bilal Ahmed Siddiqui for his treasured time, practical knowledge, advice and support which made this project possible.

We would like to thank

- Mr. Obaid Rahmani, Mr. Anas Iftikhar and Mr. Shan for their expertise and help in manufacturing and automation.
- Mr. Abid and Mr. Bilal for providing us with the testing facility.
- HEJ Center of Chemical and Biological Sciences, University of Karachi for chemical characterization of wax composition.
- Lab assistant Mr. Faraz, Mr. Farhan, and others who allowed us to use the lab equipment and other facilities in DHA Suffa University.

Finally, we would like to pay high regards to the Head of Department Dr. Muhammad Nouman Qureshi and Vice Chancellor Dr. Sarfraz Hussain for their endless support and encouragement.

Chapter 1: Introduction

A hybrid rocket motor is a bipropellant rocket engine which is an intermediate between a solid motor and a liquid engine. One of the propellants, usually the fuel, is stored as a solid grain in the combustion chamber. The other, usually the oxidizer, is stored as a liquid in a separate tank. This arrangement has an intermediate set of advantages and disadvantages, compared to solid and liquid propulsion. Compared to solid motors the main advantages of hybrids are the possibility of throttling and re-start and enhanced safety and reliability. Compared to liquid motors, the main advantages are the overall lower cost, and better engine mass fraction

The defining feature of the proposed engine is that the oxidizer is injected in the combustion chamber at the gaseous phase, rather than as liquid droplets. This is expected to enhance and stabilize combustion, as well as greatly simplifying the injector design.

1.1 Motivation

Hybrid rocket propulsion, although not a new concept, but have gathered more attention in recent years. The Hybrid Rocket is an emerging technology and there's a lot to be discovered in this field, therefore it attracts the attention of keen minds. It also engulfs mechanical engineering in the best ways; it includes thermodynamics, materials engineering, aerodynamics, heat and mass transfer, and a lot other core mechanical subjects.

One of the key motivations which make it even more attractive is that Hybrid rocket motor provides a distinct safety advantages when compared to traditional rockets that are solid and liquid based hence makes it feasible to test in an open environment.

1.2 Objective

To design, optimize and fabricate a gaseous oxidizer based hybrid rocket motor by testing different fuel combinations. Determining the best blend of fuel by finding the regression rate of different combination of waxes, biofuel and HTPB acting as a solid fuel and oxygen acting as oxidizer. Developing a method similar to centrifugal casting to achieve a uniform and homogenous fuel grain.

1.3 Statement of Requirements

Title: Hybrid Rocket Engine			Issue: 01	Date: Day-March-2016
CHANGES	D/W	REF	REQUIREMENTS	
		1	Introduction	
		1.1	Preamble	
			<i>Design, Optimization and Manufacture of a Hybrid Rocket Engine.</i>	
			<i>SUPARCO has a vision of launching their GEO and LEO satellites by 2040, for which Pakistan needs affordable satellite launch vehicles. SUPARCO has recently showed interests and reached initial understanding in this project at DSU.</i>	
			<ol style="list-style-type: none"> 1. Design of the rocket propulsion system 2. Modeling and simulations 3. Manufacture of scaled prototype and exhaustive testing 	
		1.2	Scope	
			<i>SUPARCO has shown keen interest in this project for developing Pakistan's first satellite launch vehicle (SLV). Currently, the cost of making SLV is high with conventional propulsion methods of liquid or solid propulsion. Hybrid rockets are affordable and very less complex than its alternatives. Other applications like rocket assisted take-off also exist.</i>	
		1.3	Related Documents	

		1.3.1	Books and Publications
			Sutton, G.P. and Biblarz, O., " Rocket Propulsion Elements ", John Wiley and Sons, 7 th Ed., MA, 2001.
			M. A. Karabeyoglu, Greg Zilliac, Brian J. Cantwell, Shane DeZilwa and Paul Castellucci, " Scale-up Tests of High Regression Rate Paraffin-Based Hybrid Rocket Fuels ", Journal of Propulsion and Power, Vol. 20, No. 6, p. 1037-1045, 2004.
			Elizabeth T. Jens, Ashley A. Chandler, Brian Cantwell, G Scott Hubbard, and Flora Mechentel. " Combustion Visualization of Paraffin-Based Hybrid Rocket Fuel at Elevated Pressures ", 50th AIAA/ASME/SAE/ASEE Joint Propulsion Conference, Propulsion and Energy Forum, 2014.
			Alessandro Mazzetti, Laura Merotto, and Giordano Pinarello, " Paraffin-based hybrid rocket engines applications: A review and a market perspective ," Acta Astronautica, 2016.
		1.4	Definitions, Abbreviations and Symbols
		1.4.1	Definitions
		1.4.1.1	Hybrid Rocket Engine
			Rocket engine where the fuel is in solid state and oxidizer is in liquid/gaseous state
		1.4.1.2	Choked Flow
			A condition in which the minimum area of the nozzle cannot pass more than a certain mass flow for the given conditions even if the back pressure is reduced
		1.4.1.3	Oxidizer
			Source of oxygen, not necessarily elemental oxygen
		1.4.1.4	Fuel
			A source of energy-dense hydrocarbon
			Abbreviations
		1.4.2	SUPARCO= Space & Upper Atmosphere Research Commission
			ISP= Specific Impulse
			SLV= Space Launch Vehicle

			LEO= Low Earth Orbit
			GEO= Geosynchronous Earth Orbit
			RATO= Rocket Assisted Takeoff
			Symbols
	1.4.3	D	Demand (A mandatory requirement)
		W(H)	Wish high (A highly desirable attribute)
		W(L)	Wish low (A low desirable attribute)
		W(I)	Wish Impossible (An attribute impossible without funding)
			Technical Requirements
	2		<i>Thermodynamics, Gas Dynamics, Aerospace Propulsion, Materials Engineering, Mechanics of Materials, Heat and Mass Transfer</i>
			Description & Purpose
	2.1		<i>Design, model, simulate, optimize a Hybrid Rocket Engine for requirements set by the team</i>
			<i>Satellite launch, RATO (rocket assistant take-off)</i>
		2.1.1	Functional Characteristics
	D	2.2	The rocket will be throttle able and restart able
	D	2.2.1	Design, Simulate and Optimize
	D	2.2.2	Manufacture and test scaled motors
	W(H)	2.2.3	Testing of different combinations of fuels and oxidizers
	W(I)	2.2.4.1	Manufacture and test full scale prototypes
	W(H)	2.2.4.2	Instrumentation of thrust test stand
	W(L)	2.2.5.1	Instrumentation of rocket pressures and temperatures
		2.2.5.2	Physical and other Characteristics
		2.3	

	D	2.3.1	Optimized fuel combinations
	W(H)	2.3.2	Swirl flow injectors
	W(H)	2.3.3	Nozzle insert of highly thermally stable material
		2.4	Design & Construction
		2.4.1	The main components of the Hybrid Rocket are
			<ul style="list-style-type: none"> • The oxidizer tank • The Injector • Combustion Chamber • Fuel and port geometry • Pre- and post- combustion chamber • Convergent-Divergent nozzle
	W(L)		<i>Most sensors are locally available</i>
	W(L)	2.4.3	<i>Manufacturing will be carried out indigenously</i>
	W(H)	2.4.4	<i>Testing various combinations of fuel components</i>
	W(I)	2.4.5	<i>Advanced instrumentation and full scale manufacturing</i>
		2.5	Environmental Conditions
	W(L)	2.5.1	<i>The rocket can function in air and space</i>
		2.6	Reliability & Maintenance
	W(H)	2.6.1	<i>The rocket engine requires no maintenance and can be reused</i>
		2.7	Safety
	W(H)	2.7.1	<i>Rocket is safe when operated with prescribed procedure</i>
	W(H)	2.7.2	<i>All plumbing will be leak proof.</i>
		3	Quality
		3.1	<i>The project process should be monitored by means of weekly project meetings.</i>
		3.2	<i>The project plan should be monitored by means of a Gantt chart.</i>

		3.3	<i>The chosen design should be presented at the concept design board.</i>	
		3.4	<i>The chosen design should be assessed by SUPARCO experts</i>	
		3.5	<i>The technical details should be scrutinized before detailed design work is undertaken by means of the design review board.</i>	
		4	Miscellaneous	
		4.1	<i>The Project Content will be monitored by the project advisor Dr. Bilal Siddiqui</i>	
		4.2	<i>M. Khizar Siddiqui is the project lead</i>	
		5	Costs	
		5.1	<i>The estimated cost of the Project is PKR 500,000/- approx.</i>	
		5.2	<i>The above mentioned cost is subjected to material cost, sensor requirements, testing and calibration.</i>	
		5.3	<i>The project has been approved for support by SUPARCO</i>	
		5.4	<i>In case of unavailability of funds, W may not be achieved.</i>	
		6	Constraints	
		6.1	<i>Cost and Funding are the major constraints of the project</i>	
		6.2	<i>Advanced materials and processes are expensive, but alternatives exist</i>	
		6.3	<i>Some sensors are expensive, but not all parameters need to be measures</i>	
Project Advisors/Co Advisors		Dr. Bilal A. Siddiqui		

Chapter 2: Literature Review

The propulsion team from the Mechanical Engineering Department - University of Brasília (LEA-UnB) is conducting research in hybrid rockets for a couple of years. More recently, the propulsion group has been investigating a new type of solid fuel, paraffin, whose regression rate is three to four times faster than conventional hybrid fuels, such as HTPB. The rocket used paraffin as the solid fuel and nitrous oxide as the oxidant capable of reaching 20000 meters.

Positive aspects of this idea is the ability of thrust magnitude control and restart of the motor, which influence on safety and application range. Moreover, the structure of a rocket involving a hybrid motor is not as complex as with liquid engine. It makes the hybrid less expensive and offer better performance than solid rockets.

The present development tendency of a rocket propulsion, apart from cost reduction, requires the application of environmentally friendly propellant. The Warsaw University of Technology and the Institute of Aviation conduct their own research on environmentally safe propulsion systems. The experimental hybrid rocket motor has been designed and manufactured. There have been performed several fire tests in order to verify the main properties of the propellant composition applied in the motor. The most suitable composition designed aluminum powder, ammonium nitrate, HTPB and additives: dioctyl adipate, ammonium dichromate and carbon. Aluminum increases combustion temperature. Ammonium nitrate was chosen because of its nontoxic decomposition products, low cost and high value of heat of decomposition. HTPB is the most common binder applied to solid rocket fuel grain since its high performance.

A paper submitted in 18th International Congress of Mechanical Engineering at COBEM 2005 regarding the regression rates of paraffin based hybrid rockets states that.

"Hybrid motors have regained attention for future applications in aerospace science. Because standard hybrid fuels have limited combustion velocities, such engines are not used commercially for space application. The use of hybrids rockets, though, may increase operational safety, decrease on site emissions as well as reduce costs over current solid fuels."

According to the thesis submitted by Space propulsion group based on using a mixtures of oxygen and Nitrous oxide as oxidizer to optimize the oxidizer.

A new class of oxidizers (Nytrox) which are composed of equilibrium or non-equilibrium mixtures of nitrous oxide and oxygen are formulated in order to maximize the benefits of the pure components while retaining their practical advantages. Note that in the mixture O₂ serves as the pressurizing agent, whereas N₂O is the densifying component. The primary advantages of this new system over the pure oxidizers can be listed as

- 1) self pressurization capability
- 2) high density and density impulse
- 3) non-cryogenic operational temperatures
- 4) higher Isp performance compared to N₂O
- 5) improved safety
- 6) efficient gas phase combustion
- 7) easier development of stable and efficient motors compared to liquid oxygen due to the exothermic decomposition of the N₂O molecule. Unlike the pure oxidizers, the mixture allows for two independent control variables (temperature and pressure) which can be fine tuned to optimize the system for a particular application.

Chapter 3: Design and Methodology

3.1 Fuel Grain Composition

The fuel grain is composed of different types of waxes with different percentages the purpose of which is maximize the regression rate and attain high temperatures also we use different chemicals with less percentages just to increase the melting point of wax. Different compositions of fuel grain by trial and error on few small hybrid rocket engines the purpose of which is only to measure the regression rate and the temperature which has been achieved by the engine. Different fuel combinations were tested which will be discussed in the later section.

The components of the fuel are as follows.

3.1.1 Paraffin Wax

Paraffin wax are generally available waxes, these are used in candles though there are different grades of paraffin wax. Paraffin wax is soft solid at room temperature and begins to melt at approximately 46 degrees. It is available either in white pallets. Paraffin is translucent. The density of paraffin is 900 kg/m³. Its heat of combustion is 42 kJ/g.



Figure 3-1 Paraffin Wax

3.1.2 Microcrystalline Wax

Micro Crystalline wax is a refined mixture of solid, saturated aliphatic hydrocarbons. Micro crystalline wax differ from refined paraffin as the molecular structure is more branched and it has a higher molecular weight. Micro crystalline wax is tougher more flexible and generally higher in melting point than paraffin. Microcrystalline wax is opaque. The crystal structure of microcrystalline also enables it to bind solvents or oils and act as a fuel with a higher Carbon number. The melting range of Microcrystalline is from 62 to 102 degrees.



Figure 3-2 Microcrystalline Wax

3.1.3 Poly ethylene wax

Polyethylene wax is a low molecular weight polyethylene consist of ethylene monomer chains. Polyethylene wax has a linear molecular structure as compared to other petroleum waxes. Which result in high melting point, high hardness and at an elevated temperature its melting point is around 108-115 degrees.



Figure 3-3 Poly ethylene wax

3.1.4 Carnauba wax

Carnauba is a wax of the leaves of the palm. It is the hardest among all the other waxes. It has a melting point of 82 degrees.



Figure 3-4 Carnauba wax

Further Bees wax and stearic acid was also added in order to increase the melting point, thus increasing the exhaust temperature.

3.2 Fuel Testing Engine

A new small cylinder has been manufactured with proper calculations in order to study the flame geometry, calculate the average regression rate and the flame temperature of different combination of waxes, on the basis of which the selection of the fuel is to be done.



Figure 3-5 Fuel Testing Engine

This engine consists of a graphite nozzle and an injector. The rest of the rocket is made of Mild Steel

3.3 Fuel Compositions

Every type of wax has its advantages and disadvantages due to which we cannot mold a fuel out of single type of wax. If we take Carnauba as the essential fuel it burns the best out of all the other types of waxes but due to its hard properties it cannot be molded into a single shape the wax will crack therefore it is necessary to use a binder with Carnauba which is microcrystalline . If we use Microcrystalline or paraffin or poly ethylene despite of having good regression rates they do not have a high melting point therefore the temperature of the fuel grain becomes a limitation therefore to maximize the advantages of the waxes it is necessary to mold them together and make an effective composition.

Fuel composition 1 was composed of only one kind of wax which was only paraffin therefore despite of having high regression rate during the fire it did not give desirable thrust readings and also paraffin wax is translucent therefore the thrust recorded was not up to the calculations.



Figure 3-6 Fuel composition 1

As it can be observed in the picture that the fuel grain is translucent and it is totally composed of simple Paraffin wax.

The picture of the test fire easily illustrates the translucent effect of wax which did not allow it to achieve high temperatures but due to the high regression rates we were able to extract 140 N of thrust

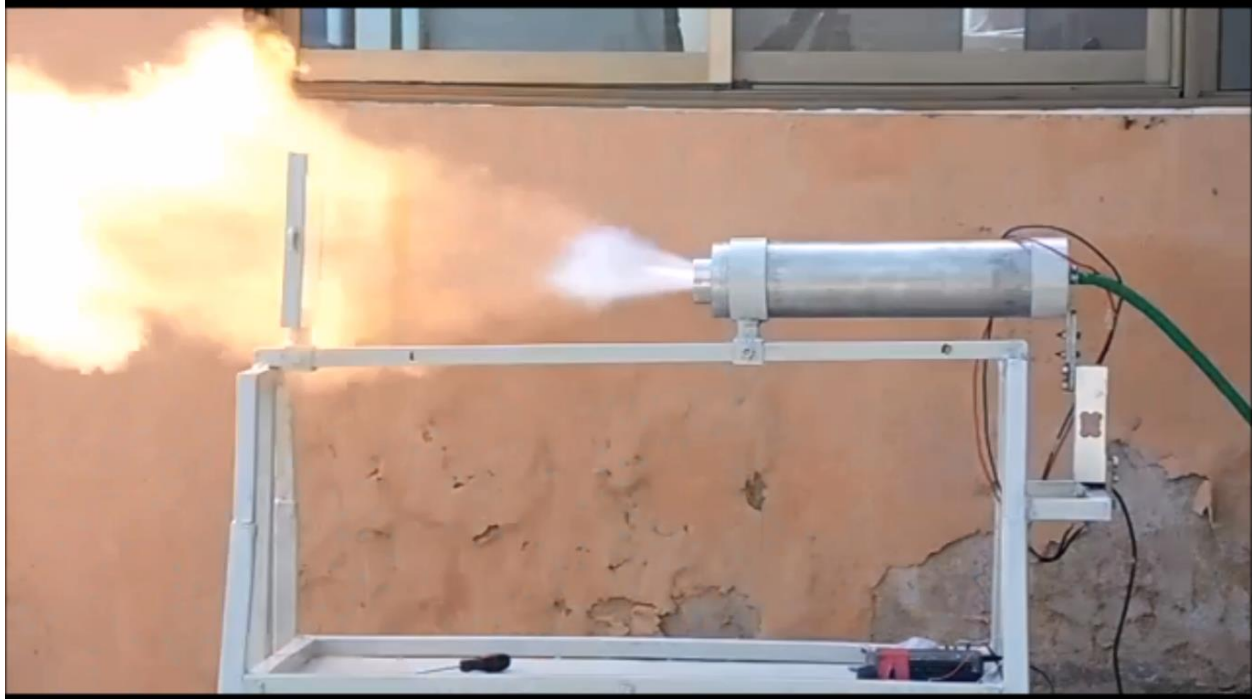


Figure 3-7 Test on Fuel composition 1

Table 1: Fuel Composition 2

Additives	Composition	Reason
Paraffin wax	94%	To maximize the regression rate
Carbon black	4%	To reduce radiation
Aluminum powder 40 micron	2%	To enhance flame geometry

The fuel grain obtained using this composition was black in color so the radiation was significantly reduced.



Figure 3-8 Fuel composition 2

The fire due to the added carbon black and aluminum powder was a successful one but due to the density difference and air pockets the translucent effects were seen at the end.



Figure 3-9 Test on Fuel composition 2 a

The effects of air pockets and translucent paraffin wax can be seen in the image



Figure 3-10 Test on Fuel composition 2 b

These were the reasons that we worked on the combination of waxes

Table 2: Fuel Composition 3

Wax	Composition	Reason
Carnauba wax	30%	To increase the flame temperature
Microcrystalline wax	30%	To act as a self burning binder
Paraffin wax	20%	To increase the regression rate
Polyethylene wax	16%	To increase the hardness
Carbon black	2%	To reduce the radiation due to its black colour
Stearic acid	2%	To increase the melting point of the mixture

This composition did not work well as expected, since the regression rate of the wax not as high as expected, also the binder was in less percentage.



Figure 3-11 Test on Fuel composition 3

As illustrated in the picture the fuel is burning outside the cylinder further it took 30 seconds for the fuel to be completely burnt further the average regression rate of 0.016 in/s.

Table 3: Fuel Composition 4

Wax	Percent composition	Reason
Microcrystalline wax	60%	To act as a self-burning binder
Paraffin wax	18%	To increase the regression rate
Polyethylene wax	18%	To increase the hardness
Carbon black	2%	To reduce the radiation due to its black colour
Stearic acid	2%	To increase the melting point of the mixture

This wax composition was designed to give a higher regression rate as it did, the regression rate this composition gave was averaged out to be 0.04 in/s.



Figure 3-12 First Test on Fuel composition 4

As this composition was successful we fired it twice to validate the result.



Figure 3-13 Second Test on Fuel composition 4

The next fire was also as much effective as before it gave a reasonable regression rate giving a pretty reasonable flame temperature the composition was then decided to be fired on the lab scale model the mold of the lab scale can be seen in the picture.

Table 4: Fuel Composition 5

Wax	Percent composition	Reason
Carnauba wax	10%	To increase the flame temperature
Microcrystalline wax	60%	To act as a self-burning binder
Paraffin wax	20%	To increase the regression rate
Polyethylene wax	16%	To increase the hardness
Carbon black	2%	To reduce the radiation due to its black colour
Stearic acid	2%	To increase the melting point of the mixture



Figure 3-14 Fuel composition 5

This composition was the best with respect to both flame geometry temperature and regression rate. This composition fits the requirements of both higher flame temperature and high regression rates.

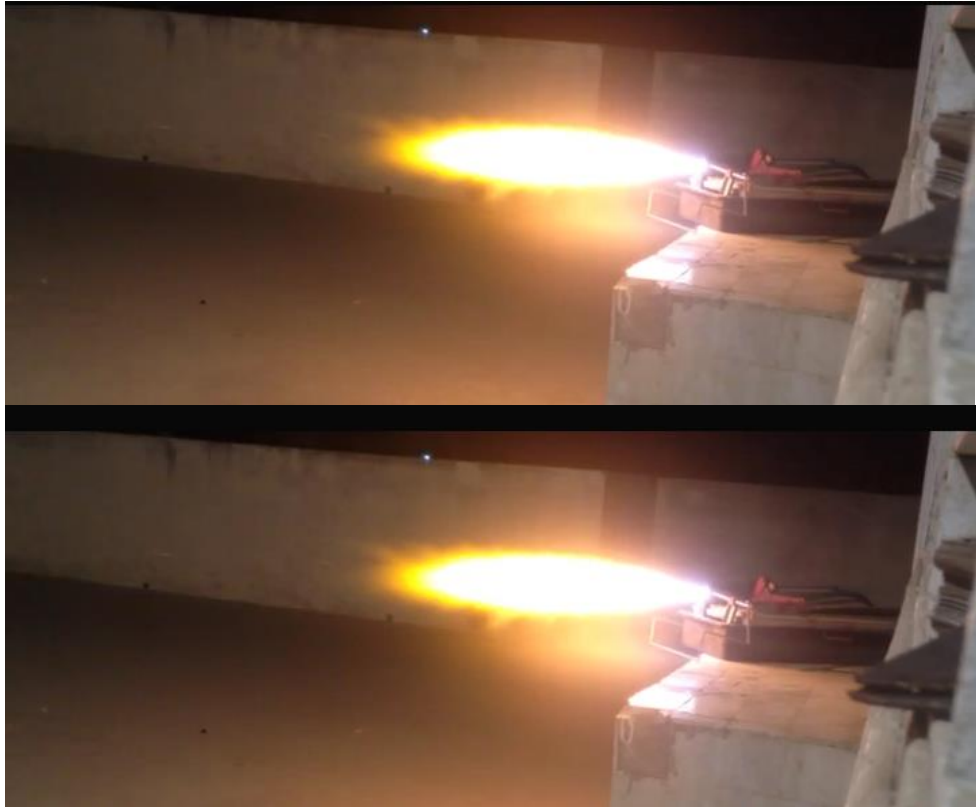


Figure 3-15 Tests on Fuel composition 5

3.4 Fuel Tests Result

The sole purpose of these tests were to obtain a fuel grain that would give a high regression rate and high flame temperature, The best candidate was the composition 5 and therefore we used it as the fuel of the rocket engine. The results obtained were promising, the average regression rate we obtained was around 0.2in/s this made sure that mass flow of the exhaust increase as much as it is required to choke the nozzle and give the maximum mass flow possible hence delivering the max amount of thrust which was around 5000 N.

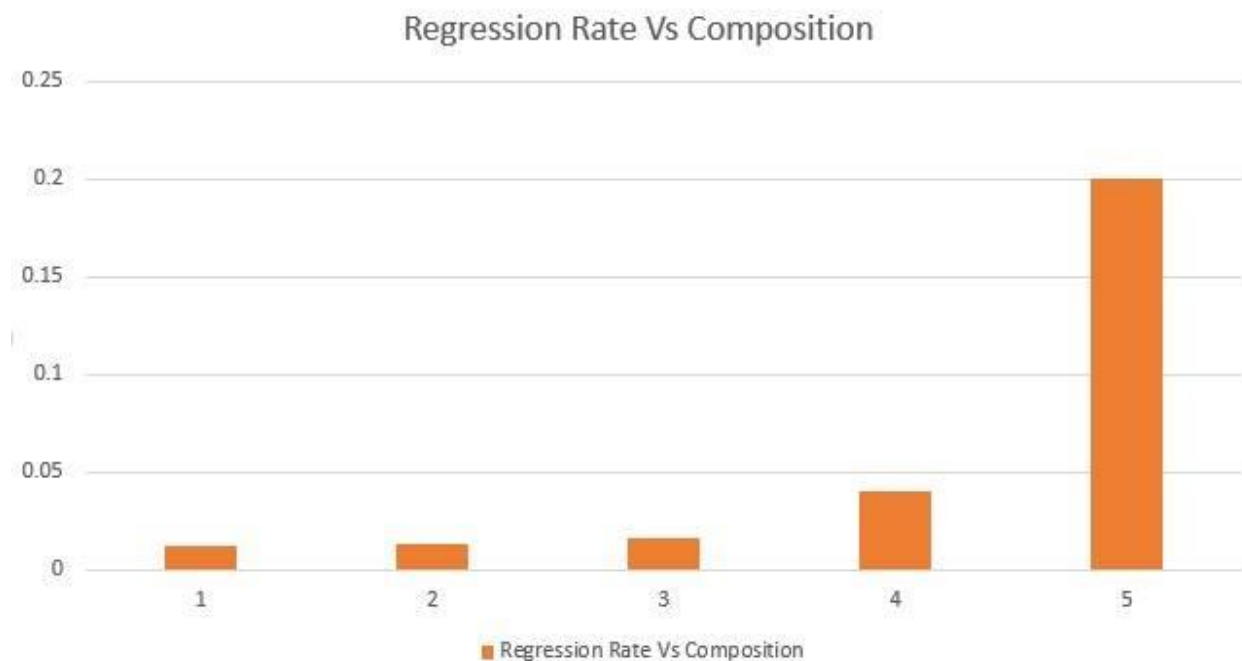


Figure 3-16 Regression Rate Comparison

3.5 Grain Manufacturing

3.5.1 Limitations

Cracks or Voids

By the analysis of the previous tests we have come to the conclusion that grain fabrication is the most critical part of the rocket engine. The possibility of presence of cracks or air pockets either on the surface or internally can lead to a catastrophic failure at high pressures and temperature and certain measures are unavoidable in order to achieve a successful test fire. The reasons of these surface or internal failure of homogeneity of the mold are because

1. Liquefied wax tends to form internal void
2. Volumetric shrinkage about 15-25% when transition from liquid to solid.

This causes a pressure gradient within the exhaust and non-uniform burning and the phenomena in the image can be seen in these circumstances.



Figure 3-17 Irregular Burning

Settling of High Density Waxes

The combination of waxes are not completely soluble into each other therefore the density difference can cause the higher density of wax to settle down while the other lower density waxes are found at the top. This causes a phenomena called end burning furthermore due to the different melting temperature of different waxes if we melt them together they can never be in the same composition as they were added some of the low melting point waxes do evaporate but due to the less percent of it we can neglect that or increase the percent composition of low melting point wax. In the following image the settling of the denser waxes can be seen.



Figure 3-18 Non-Homogeneity of Waxes

3.5.2 Solution

The solution that came up regarding the voids/cracks issue is to pressurize the liquefied mixture of the waxes using a piston with a small opening to let the trapped air pass through it. It will also be made sure that constant pressure is applied on the piston because if the pressure is not uniform, it can cause cracks with in the mold.

To solve the issue of the density difference we are going to spin the mold horizontally when it is in molten form, so that the denser wax does not settle down.

3.5.3 Methodology of Molding

The combustion chamber itself was used as the mold, it was filled with the molten composition of wax. In order to seal the wax in the chamber, two silicon plastic end caps were used with the same threads as the chamber to prevent leakages and seal the chamber. A small vent in one of the end cap was left open for the air to escape and make sure there were no air bubbles left in the mold.

The most strenuous task was to cater a 1.5 inch diameter port in the fuel grain, to allow the flow of oxidizer. To achieve this, a 1.5 inch diameter mandrel was introduced in the chamber before pouring the molten wax. Alignment of the mandrel was achieved by introducing steps in the end cap, where it would rest. A shaft was welded on top of the mandrel to align the pipe while tightening the end caps.



Figure 3-19 Mandrel

In the following figure, complete molding assembly can be seen, which consisted of a mandrel sandwiched between end caps. One of the end caps consisted of a thru-hole through which the MS shaft goes, once inserted, the hole is sealed with hot glue. Further the end caps consisted of two other holes through which the cap can be gripped and tightened. In order to release the air present, another hole was drilled on one of the caps.



Figure 3-20 Molding Assembly

Figure 3-21 shows the tightening of mold using the slots and the overflow of wax indicating that all air has escaped.



Figure 3-21 Left: Mould Pressurization; Right: Wax Overflow

Next, the chamber was mounted onto the lathe machine. It was well centered and rotated at uniform 85 rpm. Due to the unavailability of a steady rest, a custom made wooden jig was used to avoid the harmonics of the tube. Rotation at uniform rpm made sure that the mould is evenly cooled and the components are uniformly distributed. This method is called ‘Centrifugal Casting’.



Figure 3-22 Chamber Mounted on Lathe Machine



Figure 3-23 Chamber Rotating at a constant RPM on Lathe Machine

After allowing uniform cooling for 4 hours, the wax had solidified. From the appearance, the wax distribution was found to be consistent as there was no significant color change. The surface hardness was found to be even too.



Figure 3-24 Top of the Solidified Mould



Figure 3-25 Bottom of the Solidified Mould

3.6 Oxidizer tank

There were a total of four cylinders used. All the cylinders were of the same volumes and pressures (1500 psi). The cylinders were connected via stainless steel connectors which led to the stainless steel ball valve. Four cylinders were used to achieve propellant mass flow of 1.3Kg/s, which couldn't have been achieved by a single or dual cylinder combination.



Figure 3-26 Cylinder Assembly

3.7 Pipes and Fittings

The sole purpose of the pipes were to carry the propellant from the cylinders to the injector. Since the pressures and the mass flow were quite high, metal wires reinforced pipes were used with a service pressure of 88 bars. They were crimped onto the stainless steel attachments. A section of 2.5 ft. pipe crimped with attachments would go into the cylinders, while the other side of the pipe would be attached with the connectors. A further pipe attachment through the T would connect the ball valve which would go directly to the rocket engine. **Figure 3-26** shows the attachments and the order that they are to be connected together.



Figure 3-27 Attachments

Figure 3-27 shows the Pipes that were used.



Figure 3-28 Pipes Rating

The Ball Valve was rated at 170 Bars.



Figure 3-29 Ball Valve

The connectors were rated at 120 Bars.



Figure 3-30 T-Connectors

3.8 Igniter

As a result of this inherent propellant stability, hybrid motors have historically proven difficult to ignite. So in order to achieve this multiple consecutive ignitions were performed. Since this is an original groundwork research project, concepts have been developed about a reliable, operational igniter system.

High Current-gasoline was used initially used that involved Ignition of hybrid rocket motors by passing high current through ni-chrome wire wrapped around a combination of cotton and match powder soaked in gasoline. In an oxygen rich environment to ignite the fuel and oxidizer. This ignition method makes use of an external gaseous oxygen supply to fill the combustion chamber with gaseous oxygen. High current is then passed through a ni-chrome placed at the injector end of the combustion chamber, causing thermal breakdown of the resistance coil. The coil heats up white hot, causing the cotton match powder mixture to ignite. Since the match powder has a slow response to heat, this setup didn't come off most of the time. Also the low boiling point of gasoline caused fumes to accumulate in the chamber resulting in a small blast.

Then a new, much more reliable igniter was formulated that could catch fire instantly i.e. black powder.

Table 5: Ingredients of black powder

Content	% per mixture
Potassium Nitrate	60%
Sorbitol	30%
Carbon powder	5%
Sulphur	5%

Water is added to the mixture in the same amount as Potassium Nitrate which is later cooked on low flame until all the water has evaporated. Stirring is necessary during cooking. The final result would be black powder, as the name tell us. This formulation has provided us with great results every time we used it, it has worked every time we put it to test.

Since an igniter is a one-time use device, it only needs to stay hot long enough to ignite the pyrogen and that is only a split second. The igniter wire experiences extreme heat melts or vaporizes the igniter wire in one place or in its entirety.

The wire is long enough so that the igniter can be pushed all the way through the motor core to the forward end of the rocket and the other end can protrude out the nozzle. The air pressure pushes the wire out, when the oxidizer is allowed to flow.

The wire being used are 10 meters long, so the battery operator is quite safe in case of any mishap.

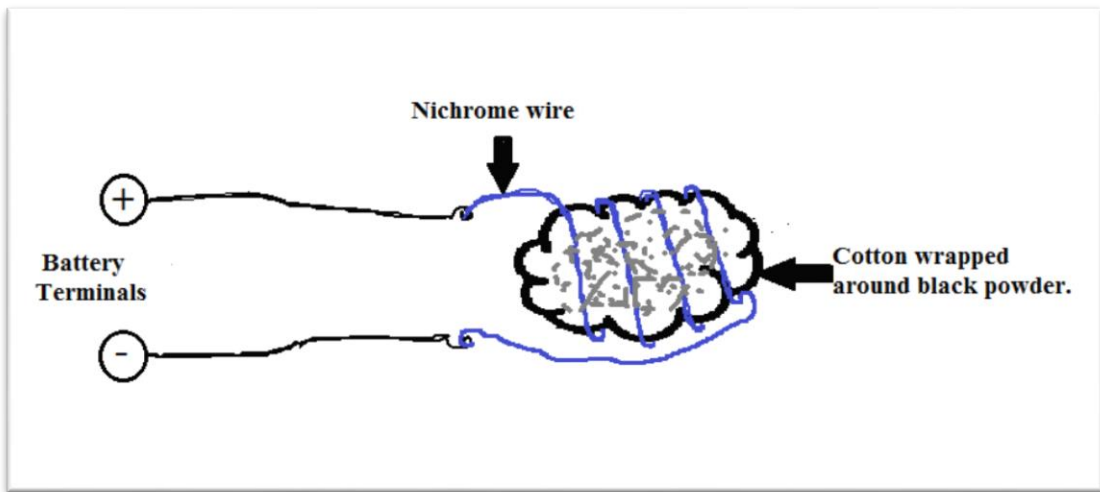


Figure 3-31 Igniter Assembly

3.9 Automating the Design Process and Analysis

3.9.1 Introduction

The rocket design process defined previously is very cumbersome if done by hand. In order to automate the process, a code was developed in MATLAB. The following sections reproduce some of the results.

All MATLAB Codes used in the simulations can be found on the following webpage for verification:

[GitHub - airbilal/Hybrid-Rocket-Engine-Design-Tool](#)

3.9.2 Inputs

The inputs to the code are collected in structures called requirements, materials, oxidizer, fuel, combustion products, and engine. Their details are given in table below.

Table 6: Description for Code Inputs

Structural Element (code)	Description	Unit
requirements.F	Required thrust	N
requirements.tb	Required burn time	S
requirements.pinj	Pressure of oxidizer at injector inlet	Bar
requirements.pexit	Nozzle exit pressure (design point)	bar
requirements.Lstar	Characteristic length of combustion chamber	m
requirements.acat	Contraction ratio, A_c/A_t	-
requirements.halfangle_con	Half angle of convergent side (45-60]	deg
requirements.halfangle_div	Half angle of divergent side [10-20]	deg
requirements.throatcurv	Ratio of curvature at throat to throat radius [0.5-1.5]	-
materials.wall.grade	Material of chamber wall	-
materials.wall.servtemp	Chamber material service temperature	K
materials.wall.strength	Tensile strength	Pa
materials.wall.fos	Factor of Safety for chamber	-
materials.wall.cond	Thermal Conductivity for wall material	W/m/K
materials.insert.grade	Material for nozzle insert [Graphite, Tungsten etc.]	-
oxidizer.name	Name of oxidizer [LOX, GOX, N2O2 etc.]	-
fuel(1).name	Name of first fuel [C8H18, RP-1 etc.]	-
combustionproduct(1).formula	Chemical formula of first combustion product [CO2 etc.]	-

engine.outside.h	Natural convection coefficient on outside surface of engine	W/m ² /K
engine.outside.Ta	Ambient temperature	K

These are defined in the main.m script.

3.9.3 Stoichiometric Calculations

Stoichiometric calculations provide the starting point for the optimization procedure. These are carried out in the stoichiometry.m script, which basically solves set of linear equations. A sample calculation is shown below for paraffin fuel ($C_{26}H_{54}$)



The stoichiometric oxidizer/fuel ratio (OFR) is then calculated as

$$OFR_{stoich} = n_{oxidizer} \times \frac{M_{oxidizer}}{M_{fuel}}$$

Where, n is the number of moles and M is the molecular weight. In our sample calculations, MATLAB gives the stoichiometric OFR = 3.45.

3.9.4 Optimizing the Oxidizer to Fuel Ratio (OFR)

The stoichiometric OFR is not necessarily the most optimal, and secondly, it varies during engine operation for most rockets. The function ofr_optim.m is used to simulate thrust and temperature with varying OFR. It calls another function called runCEA2.m, which in turn parses the input text file for NASA's Chemical Equilibrium and Analysis (CEA2) software to perform complex thermochemical calculations. CEA is a widely accepted tool in the industry and used professionally in propulsion applications. For our sample calculations, we obtain the following variations in engine performance.

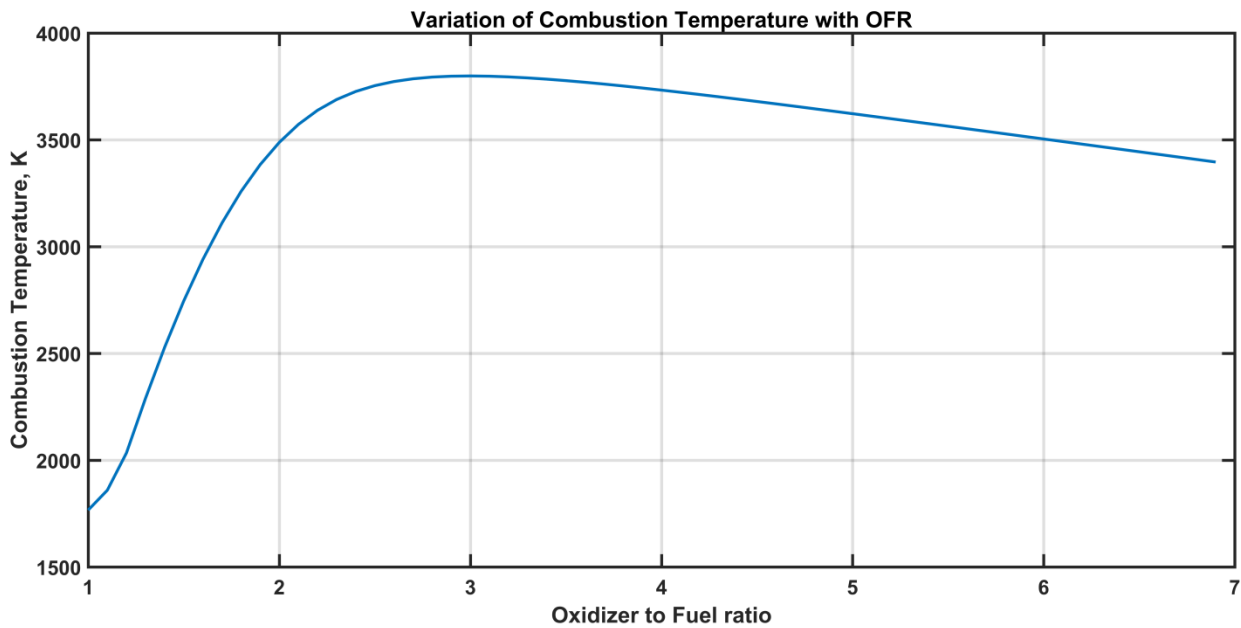


Figure 3-32 Variation of Combustion Temperature with OFR

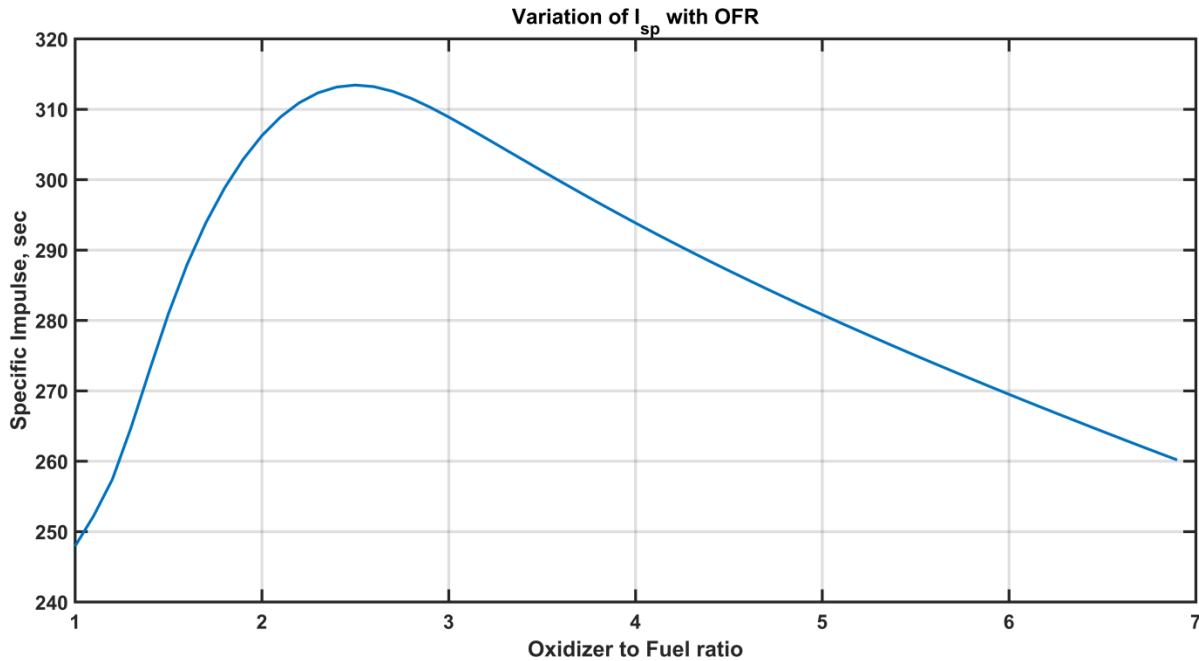


Figure 3-33 Variation in I_{sp} with OFR

This confirms that the best engine performance does not occur at stoichiometric equilibrium point. Rather, the best specific impulse (313.4 s) is obtained when the engine runs slightly fuel

rich, at OFR=2.5. However, the engine temperature is also high at this point, so perhaps a lower value of about 2 can be used. This reduces the oxidizer tank volume as well.

The function also utilizes CEA for finding the optimal nozzle throat to exit area ration, as well as nozzle Mach, Reynolds and Prandtl numbers at inlet, throat and exit. At optimal OFR (2.5), the optimal $A_e/A_t=11$ and exit Mach number is $M_{exit}=3.17$.

3.9.5 Isentropic and Heat Transfer Analyses

The function sizing_HRE.m uses the optimized values above to find major dimensions of the rocket propulsion system. Its outputs are used by functions isentrpy.m and heat_transfer.m to perform one-dimensional isentropic and heat transfer nozzle calculations at discrete nozzle locations.

3.9.6 Boundary Layer Temperature

The gas slows considerably in the boundary layer, and therefore its temperature rises above the temperature of the gas away from the wall in the free stream. It can be calculated as follows.

$$T_{aw} = T_o \left[\frac{1 + r \frac{\gamma_g - 1}{2} M_x^2}{1 + \frac{\gamma_g - 1}{2} M_x^2} \right]$$

Where, T_0 =stagnation temperature in the chamber (adiabatic flame temperature, obtained from CEA), γ_g = ratio of specific heats for gas (obtained from CEA), M_x =local Mach number, r =local recovery factor. The recovery factor is given as

$$r = \text{Pr}_g^{0.33}$$

where, Pr_g is the Prandtl number is also obtained from CEA as well. The results of this analysis are presented in Figure 3-34.

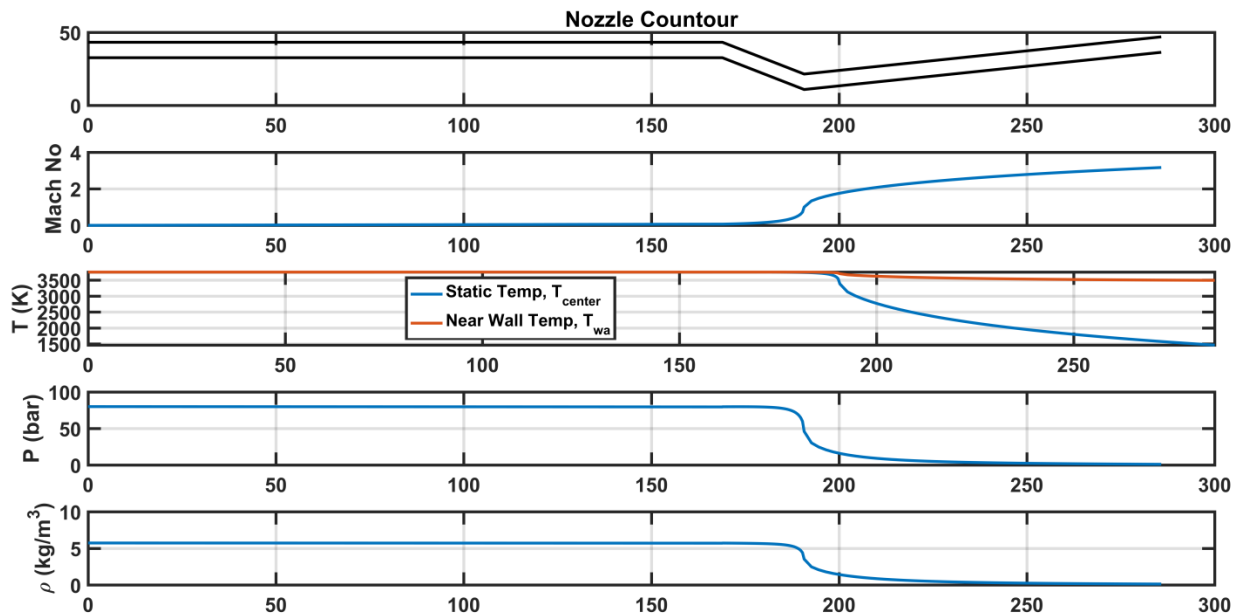


Figure 3-34 Variations of Flow Properties along Nozzle Axis

(axial locations in mm, origin 190mm upstream of throat)

3.9.7 Heat Transfer in Combustion Chamber

In the combustion chamber, the variable port diameter forms the inner wall of the fuel grain. In the chamber, the heat transfer problem is posed as shown in Error! Reference source not found.3-5 and Error! Reference source not found.3-36. Thermal circuits can be used to evaluate heat transfer and solve for unknown temperatures in this quasi-steady state setting. In this analogy with electric circuits, current is analogous to the rate of heat transfer, electrical resistance to thermal resistance, and the potential difference to the temperature difference between each node. Using material properties of the engine, fluid properties of combustion gases, and geometry, thermal resistances can be solved for unknown temperatures. Rate of heat transfer depends on transfer mode, i.e. whether conduction or convection is taking place. The following modes exist in this case.

3.9.8 Gas-side Heat Transfer

Heat transfer from the combustion gas to the fuel grain occurs by forced convection. The heat is transferred from the gas to the wall by conduction through the stagnant boundary layer. Heat transfer from the gas to the chamber wall follows the following law.

$$q_{out} = q - q_{pc} = h_g(T_{aw} - T_{fg}) - \frac{h_{pc} \dot{m}_f}{\pi d_p L_p}$$

Where, q = Heat flux across the boundary layer to the fuel (W/m^2), T_{aw} = adiabatic temperature of the gas in boundary layer (K), T_{fg} = gas side temperature of the fuel grain and h_g =gas side heat transfer coefficient ($\text{W/m}^2/\text{K}$). Some of the heat transferred is used in melting and vaporizing the fuel grain. This is heat flux for phase change q_{pc} , which is related to latent heat of the fuel h_{pc} (J/kg), fuel consumption rate and instantaneous port diameter.

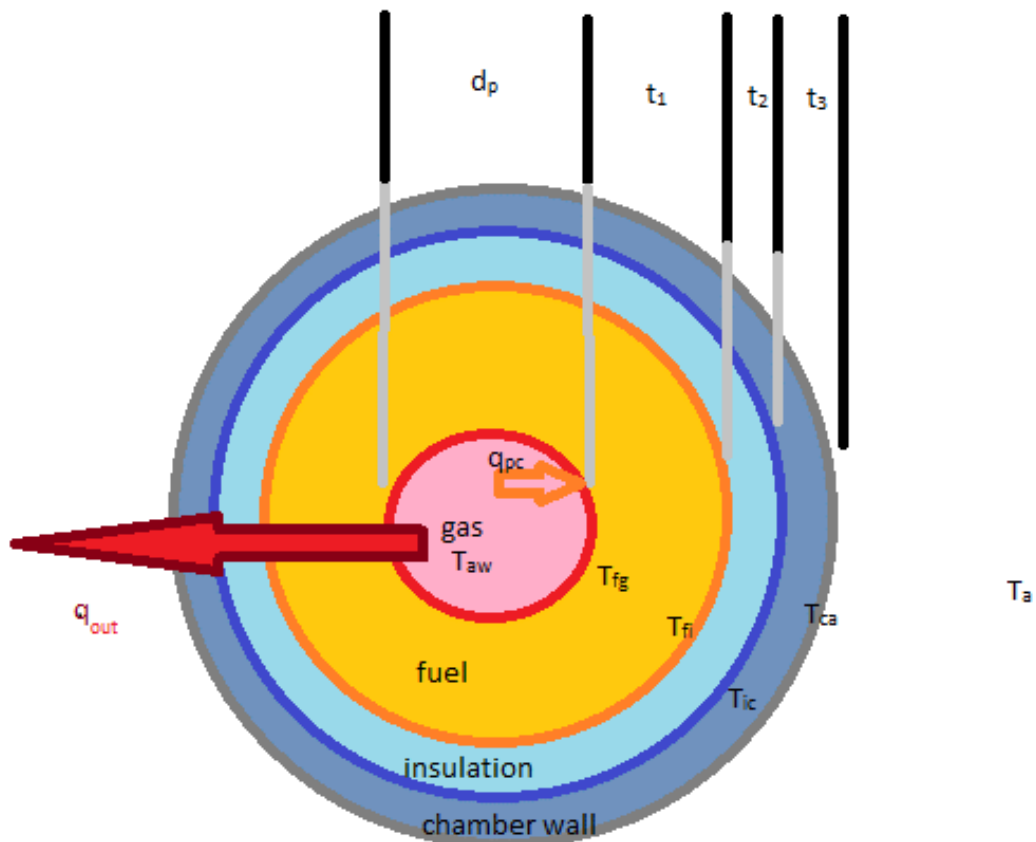


Figure 3-35 Thermal Model of Combustion Chamber

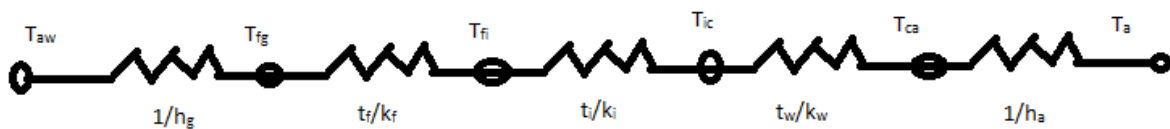


Figure 3-36 Electrical Analogy of Heat Transfer through Combustion Chamber

The gas slows considerably in the boundary layer, and therefore its temperature rises above the temperature of the gas away from the wall in the free stream. It can be calculated as follows.

$$T_{aw} = T_o \left[\frac{1 + r \frac{\gamma_g - 1}{2} M_x^2}{1 + \frac{\gamma_g - 1}{2} M_x^2} \right]$$

Where, T_0 =stagnation temperature in the chamber (adiabatic flame temperature, obtained from CEA), γ_g = ratio of specific heats for gas (obtained from CEA), M_x =local Mach number, r =local recovery factor. The recovery factor is given as

$$r = \text{Pr}_g^{0.33}$$

Where, Pr_g is the Prandtl number is also obtained from CEA as well. Prof. Bartz developed the following correlation for gas side heat transfer, based on many experiments.

$$h_g = \left[\frac{0.026}{D_t^{0.2}} \left(\frac{\mu_g^{0.2} c_{p_g}}{\text{Pr}_g^{0.6}} \right) \left(\frac{P_0 g}{c^*} \right)^{0.8} \left(\frac{D_t}{R_{curv.}} \right)^{0.1} \right] \left(\frac{A_t}{A_x} \right)^{0.9} \sigma$$

Where,

$$\sigma = \frac{1}{\left[\frac{1}{2} \frac{T_{fg}}{T_0} \left(1 + \frac{\gamma - 1}{\gamma} M_x^2 \right) + \frac{1}{2} \right]^{0.68} \left[1 + \frac{\gamma - 1}{2} M_x^2 \right]}$$

Thus, the gas side heat transfer coefficient is a function of both the diameters of throat, nozzle and chamber, as well as nozzle curvature ($R_{curv.}$) and fuel temperature on the gas side (unknown). Therefore, the system of equations is nonlinear. It also depends on chamber pressure (P_o) and viscosity (μ_g).

3.9.9 Conduction through Fuel, Insulation and Chamber Wall

This heat is then to be conducted through three layers

- i. fuel grain (conductance $k_f=0.2$ W/m/K, thickness $t_1=t_f$)
- ii. insulator (conductance $k_i=0.1$ W/m/K, thickness $t_2=t_i$)
- iii. chamber wall (conductance $k_w=169$ W/m/K, thickness $t_3=t_w$)

The thermal resistance to conduction is given as $R=t/k$. Since all of them are connected in series, the overall heat resistance is given as $R_{cond} = \frac{t_f}{k_f} + \frac{t_i}{k_i} + \frac{t_w}{k_w}$

3.9.10 Convection at the Chamber Wall

The external walls are at higher temperature than the ambient. Heat may be lost by either natural or forced convection depending on whether the rocket is statically tested or launched dynamically. Considering natural convection modeled as horizontal cylinder in still air, we assume $h_a=100 \text{ W/m/K}$.

3.9.11 Overall Heat Transfer

The overall heat transfer resistance can now be solved as

$$R_{chamber} = \frac{1}{h_g} + \frac{1}{h_a} + \frac{t_f}{k_f} + \frac{t_i}{k_i} + \frac{t_w}{k_w}$$

The corresponding heat transfer coefficient is therefore

$$H_{chamber} = \frac{1}{R_{chamber}} = \frac{1}{\frac{1}{h_g} + \frac{1}{h_a} + \frac{t_f}{k_f} + \frac{t_i}{k_i} + \frac{t_w}{k_w}}$$

The different temperatures can then be solved as follows

$$q - q_{pc} = h_g(T_{aw} - T_{fg}) - \frac{h_{pc} \dot{m}_f}{\pi d_p L_p} = \frac{T_{fg} - T_{ac}}{\frac{t_f}{k_f} + \frac{t_i}{k_i} + \frac{t_w}{k_w}} = h_a(T_{ac} - T_a)$$

The port diameter changes as (where d_{p0} is initial fuel port diameter and \dot{r}_p is fuel regression rate

$$d_p = d_{p0} + 2\dot{r}_p$$

Temperatures T_{aw} and T_a are known to us due to foregoing. Similarly all thickness, conductivities and h_a are also assumed to be known. The great unknown is T_{fg} which also enters the calculations in a nonlinear fashion. The solution of these equations is outside the scope of this work, and left for future studies.

3.9.12 Heat Transfer in Rocket Nozzle

In rocket nozzle, there is fuel grain or insulator lining. Instead, heat transfer is impeded by a graphite insert, as illustrated in previous chapters. Therefore, the heat transfer is simplified, as there is no phase change. The heat transfer equations are now reduced to

$$q = h_g(T_{aw} - T_{insg}) = \frac{T_{fg} - T_{ac}}{\frac{t_{ins}}{k_{ins}} + \frac{t_w}{k_w}} = h_a(T_{ac} - T_a)$$

This is relatively simpler to solve, as there is no variable geometry and only two conduction layers exist.

3.9.13 Conclusion

This section laid the foundation for further study of heat transfer to the chamber and nozzle walls. The full solution is beyond the scope of SORs, but it sets the tone for further studies. Moreover, the assumption of one-dimensional heat transfer may not be valid in all cases and needs to be investigated further in later works.

3.10 Calculations

MATLAB screenshots:

```
t: 3.5198e+03
rho: 2.6187
mw: 25.4390
cp: 7.7984
gam: 1.1247
vis: 0
cond: 0
mach: 1.0004
cf: 0.6522
ivac: 2.1489e+03
isp: 1138
sonic: 1.1375e+03
```

Figure 3-37 Throat data from MATLAB

```
t: 3.6867e+03
rho: 4.2503
mw: 25.0550
cp: 7.6590
gam: 1.1295
vis: 0
cond: 0
mach: 0
cf: 0
ivac: 0
isp: 0
sonic: 1.1756e+03
```

Figure 3-38 Combustion Chamber Data from MATLAB

3.10.1: Nozzle

Using the MATLAB codes the Pressure inside the combustion chamber comes out to be 80 bars and the flame temperature is around 3500K.

By using the codes the ratio of specific heats come out to be 1.1247 at the throat which is used to determine the velocity.

$$v_2 = \sqrt{\frac{2k}{k-1} RT_1 \left[1 - \left(\frac{p_2}{p_1} \right)^{(k-1)/k} \right]}$$

Taking the underestimated value of temperature and by using the equation we determined the velocity to be 2412.149 m/s.

By defining the required thrust which in our case 5000N is considering the unavoidable losses it could be around 4500 N also in order to keep the mass flow rate at an acceptable value because if we overestimate the thrust the value for mass flow rate can be a non-realistic value.

$$T = mp * V$$

The required mass flow of propellants is 1.8 Kg/s

$$\dot{m} = \frac{A_t v_t}{V_t} = A_t p_1 k \frac{\sqrt{[2/(k+1)]^{(k+1)/(k-1)}}}{\sqrt{kRT_1}}$$

Using the equation we can find out the throat area that can provide enough mass flow which comes out to be 0.0004155 m² by using this area, the diameter of the throat comes out to be 23 mm. As the throat is defined, we can now determine the exit area required to provide the pressure drop at the throat temperature.

$$\frac{A_t}{A_2} = \left(\frac{k+1}{2} \right)^{1/(k-1)} \left(\frac{p_2}{p_1} \right)^{1/k} \sqrt{\frac{k+1}{k-1} \left[1 - \left(\frac{p_2}{p_1} \right)^{(k-1)/k} \right]}$$

From this equation the exit area can be easily determined which comes out to be 0.0034 m² and hence the diameter of the exit comes out to be 65.83mm Using the areas we can determine the area ratio of the con-di nozzle which is 8.183. Using this area ratio we can determine the Mach number by iterating the following equation:

$$\frac{A_y}{A_x} = \frac{M_x}{M_y} \sqrt{\left\{ \frac{1 + [(k-1)/2]M_y^2}{1 + [(k-1)/2]M_x^2} \right\}^{(k+1)/(k-1)}}$$

At the throat, the Mach number is 1 which is the designed condition of the rocket Engine therefore by iterating the equation the Mach number comes out to be 2.625.

$$Isp = \frac{Thrust}{mass\ flow * g}$$

The specific impulse is 254.80 s.

And the characteristic velocity is determined by the following equation:

$$C^* = \frac{P_c * A_t}{m}$$

Which is 1846.79 m/s.

3.10.2: Fuel

The regression rate can be assumed to 0.2 in/s to calculate the port diameter by using the regression rate constants.

a=0.276 for wax with gaseous oxygen

n=0.5

r=0.2 in/s

$$r = a \left(\frac{m_{ox}}{A_p} \right)^n$$

Solving the above equation for the port area:

$$A_p = \left(\frac{a}{r} \right)^{1/n} * m_{ox}$$

However the oxidizer mass flow rate is to be calculated through the oxidizer fuel ratio that is determined in stoichiometry and comes out to be 3.45.

$$m_{ox} + m_f = 1.8 \quad m_{ox} + \left(\frac{m_{ox}}{OFR} \right) = 1.8$$

From here the mass flow of oxidizer can be determined as 1.4 Kg/s. Mass flow of fuel is 0.4 Kg/s.

And hence the port diameter comes out to be 38.1mm.

The length of the port is to be calculated using the equation.

$$L_p = 0.83328 \cdot (OF)^{-1} \cdot (D_p)^{0.06} \cdot (\dot{m}_{ox})^{0.53}$$

The length of the port is 914.4 mm.

3.10.3: Injector

The area of the injector is dependent on the required mass flow of the oxidizer, pressure of the oxidizer, density of the oxidizer and the discharge coefficient.

$$A_{inj} = \frac{\dot{m}_{ox}}{C_d \cdot \sqrt{2 \cdot \rho_{ox,g} \cdot p_{ox} \cdot \left(\frac{2}{\gamma_{ox} + 1} \right)^{\frac{\gamma_{ox} + 1}{\gamma_{ox} - 1}}}}$$

The density of oxidizer is 4.25 Kg/m3. The pressure upstream is 80 bars and the discharge coefficient is 0.6 for the angular holes of the injector using the equation the total diameter of the injector required for such a flow is 25.4mm.

In our case, there are 14 holes for the injector therefore for each hole to provide equal mass flow, the diameter of each hole should be 6.0mm

3.10.4: Combustion Chamber

The thickness of the material should be enough to withstand the hoop stress created by the pressure:

$$t = \frac{(FOS) * (Pc * d)}{2 * Yield Stress}$$

The thickness of the chamber required at diameter 139.7 mm is 8.4mm in order to keep the factor of safety 2. Material is tempered Aluminum

3.11 Manufacturing Drawings

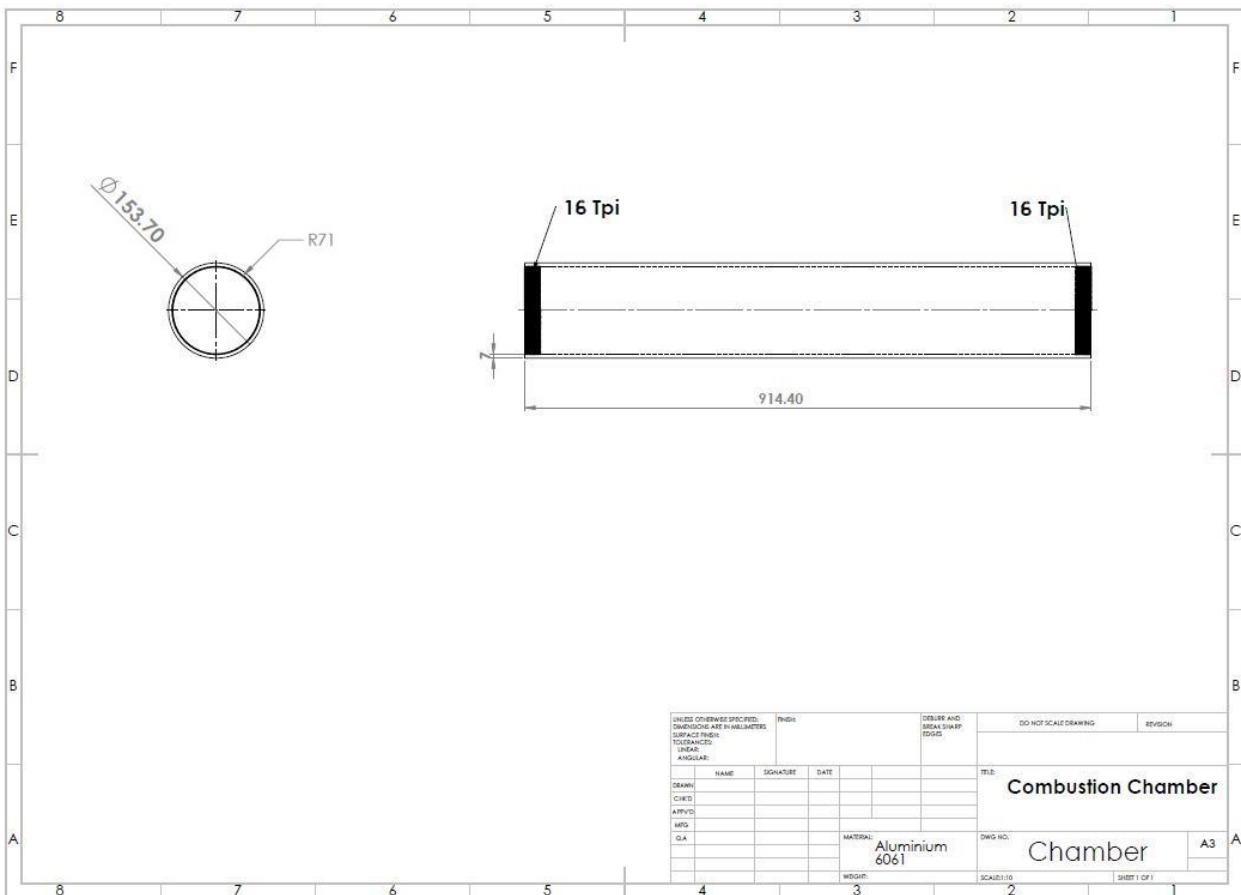


Figure 3-39 Production Drawing of Combustion Chamber

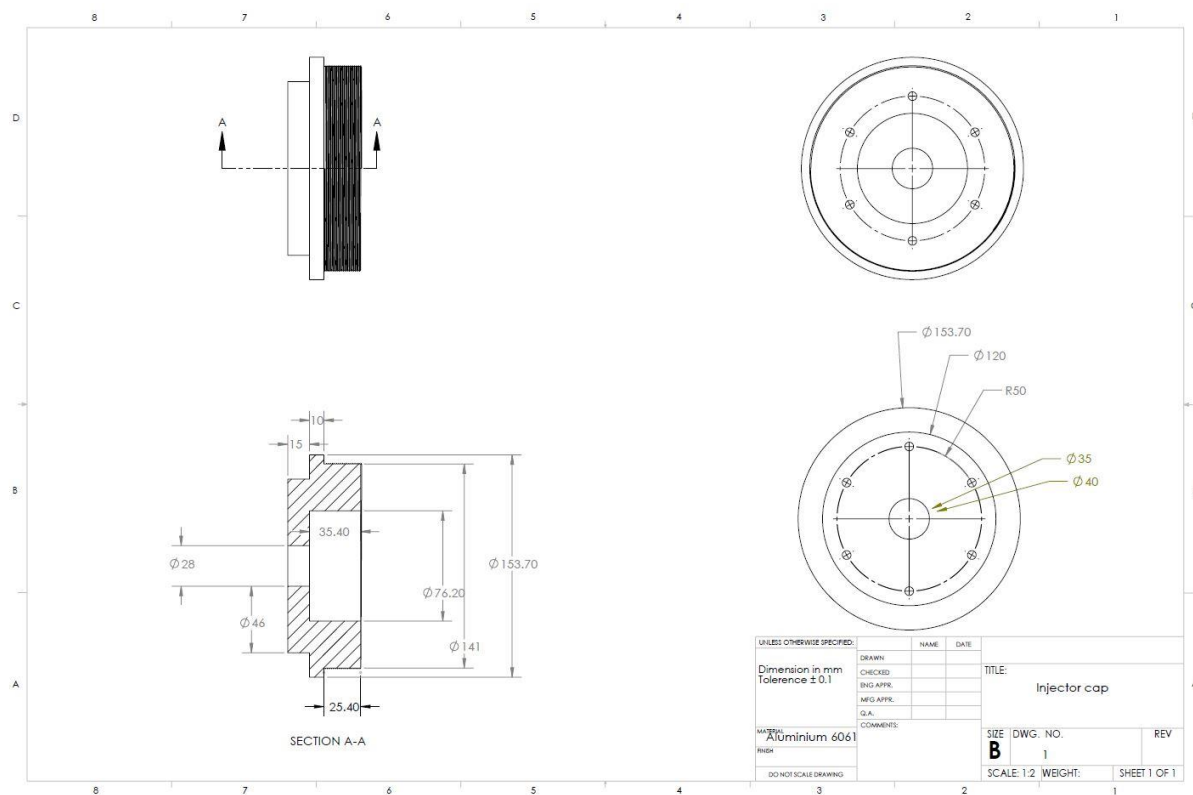


Figure 3-40 Production Drawing of Injector cap

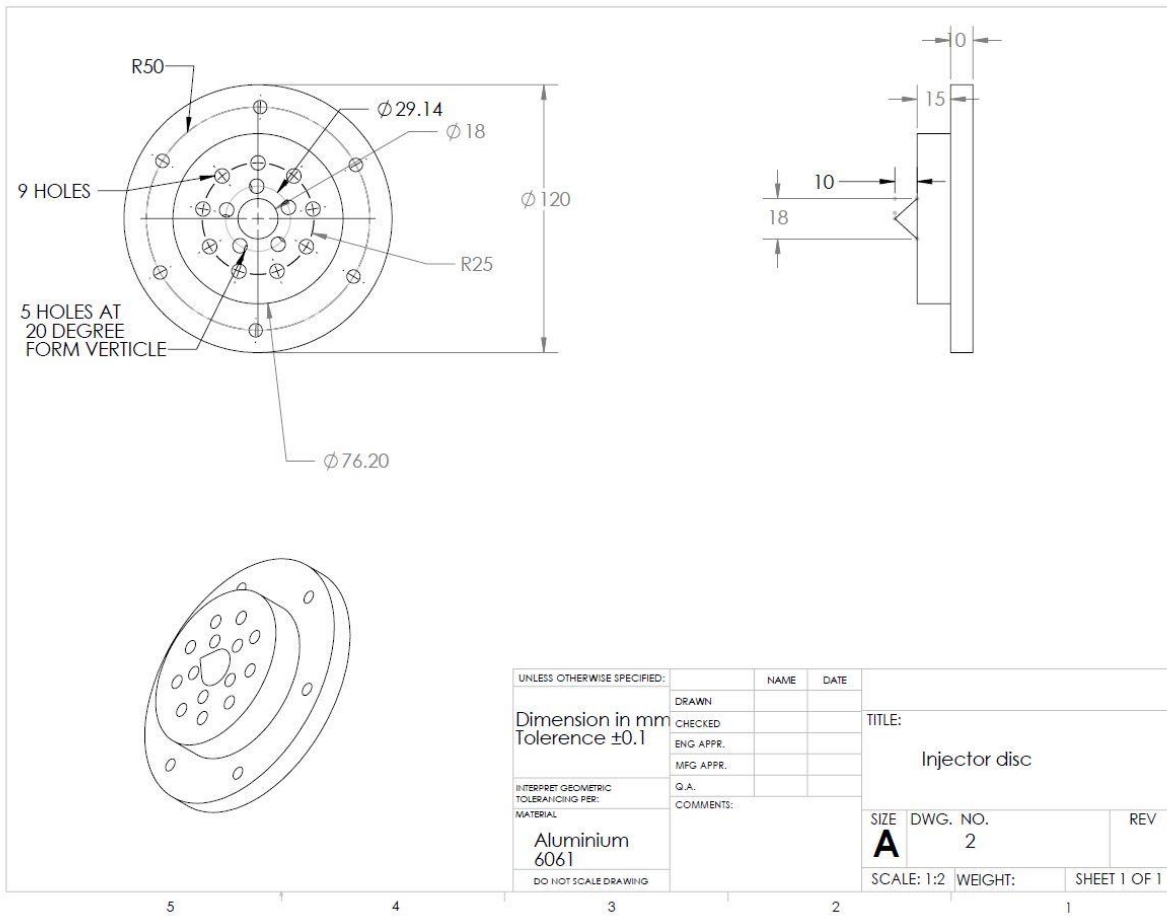


Figure 3-41 Production Drawing of Injector Disc

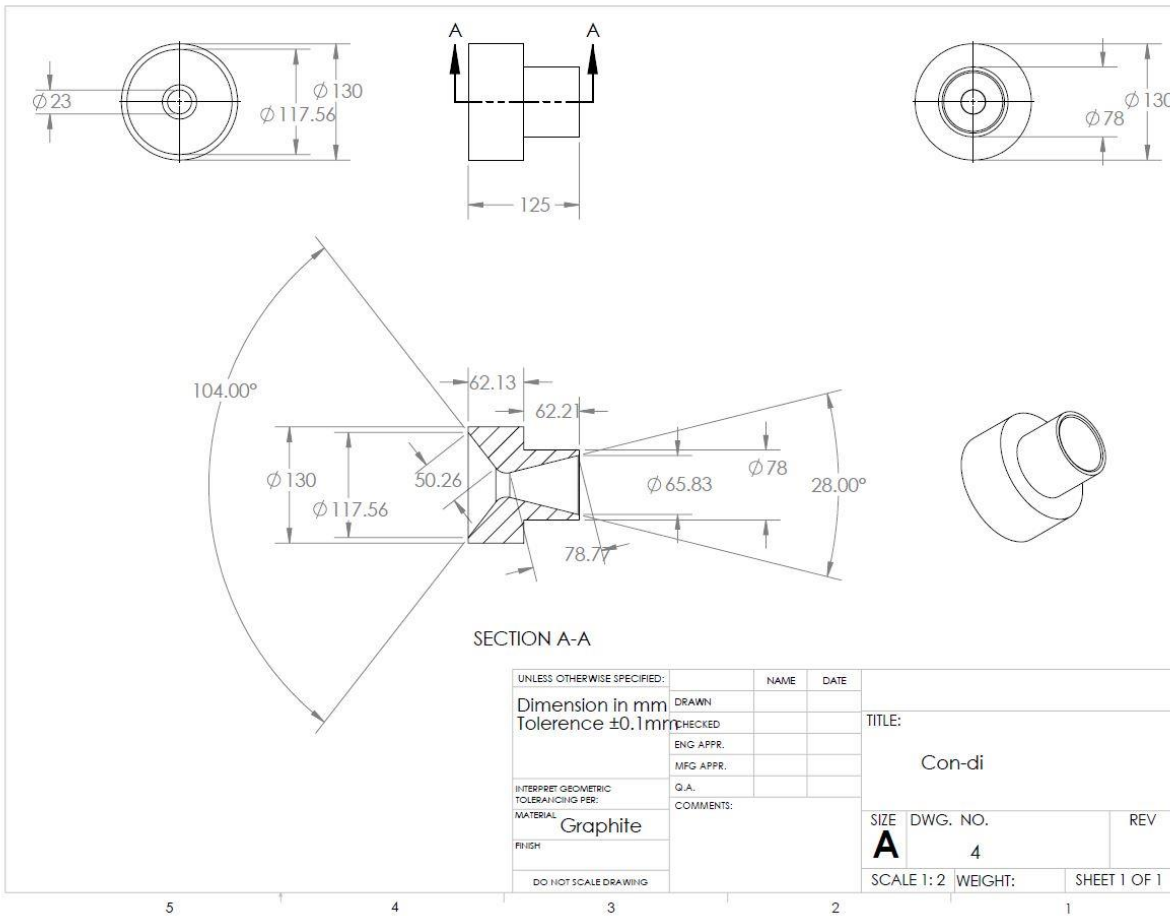


Figure 3-42 Production Drawing of Con-Di Nozzle

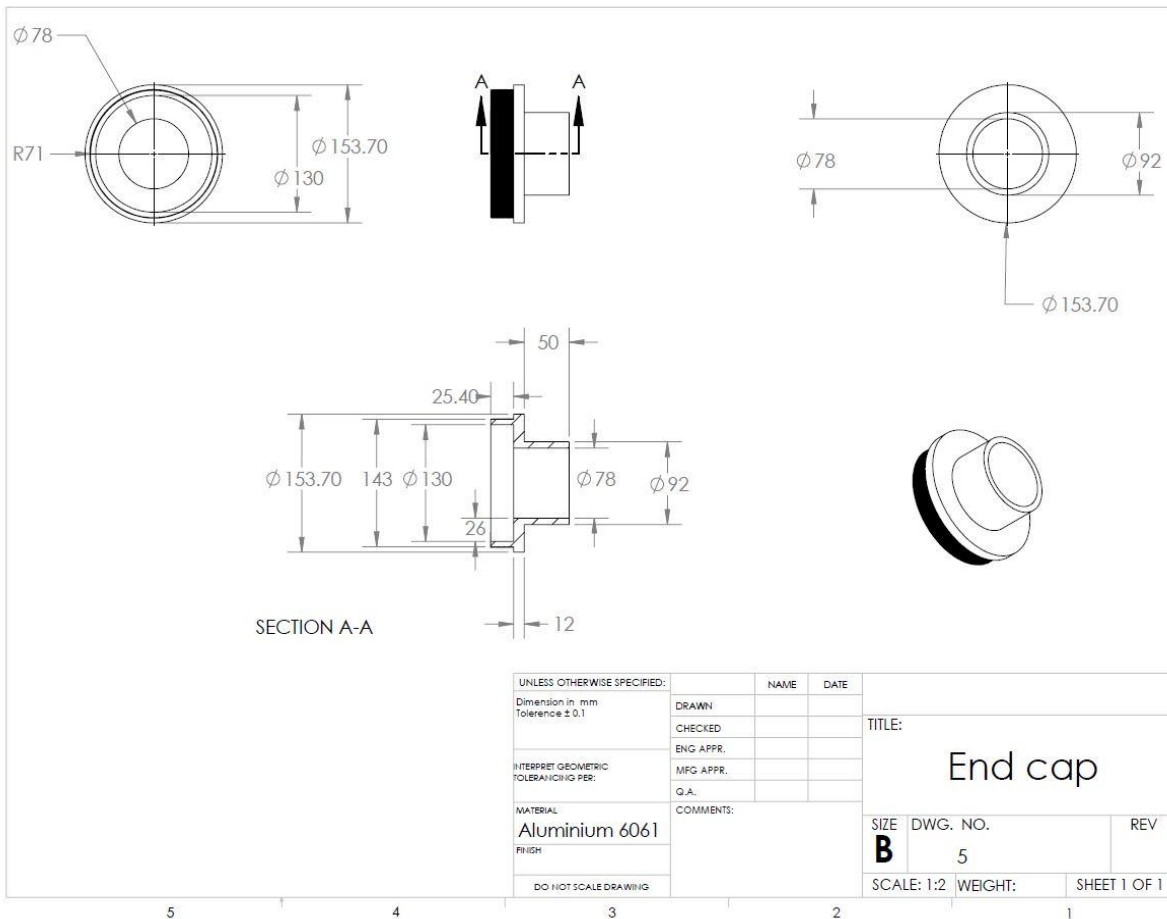


Figure 3-43 Production Drawing of End Cap

3.12 CAD Drawings



Figure 3-44 Rocket Assembly

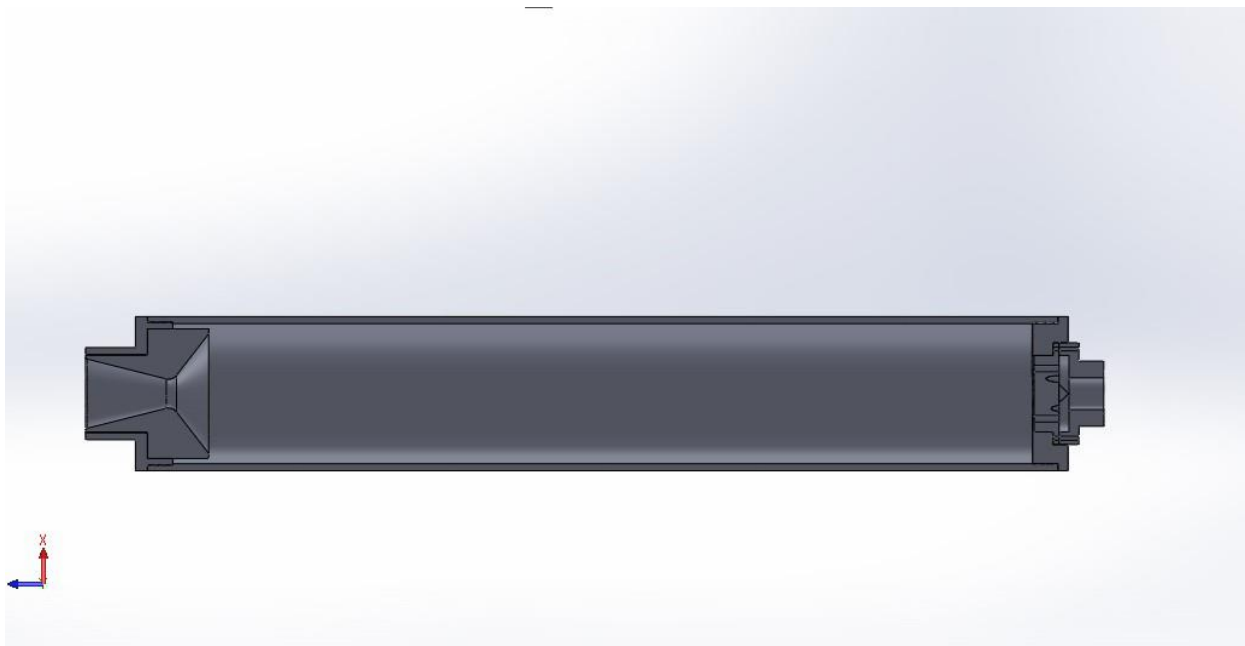


Figure 3-45 Rocket Assembly Section View

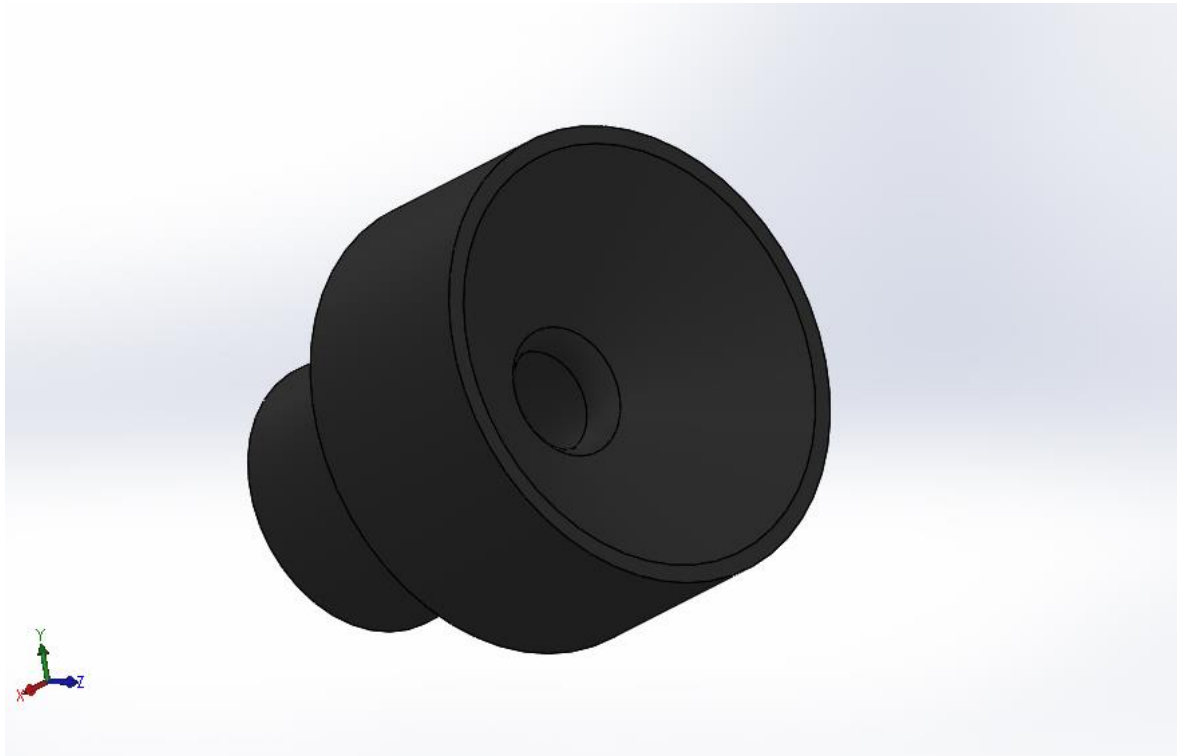


Figure 3-46 Con-Di Nozzle

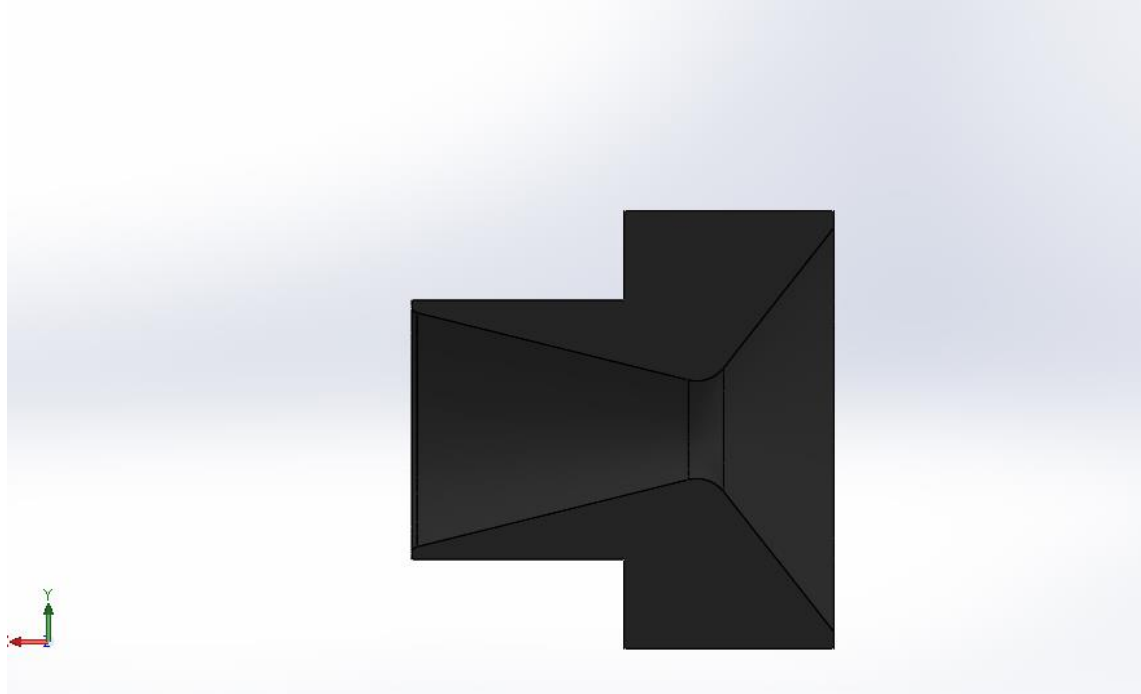


Figure 3-47 Con-Di Nozzle Section View

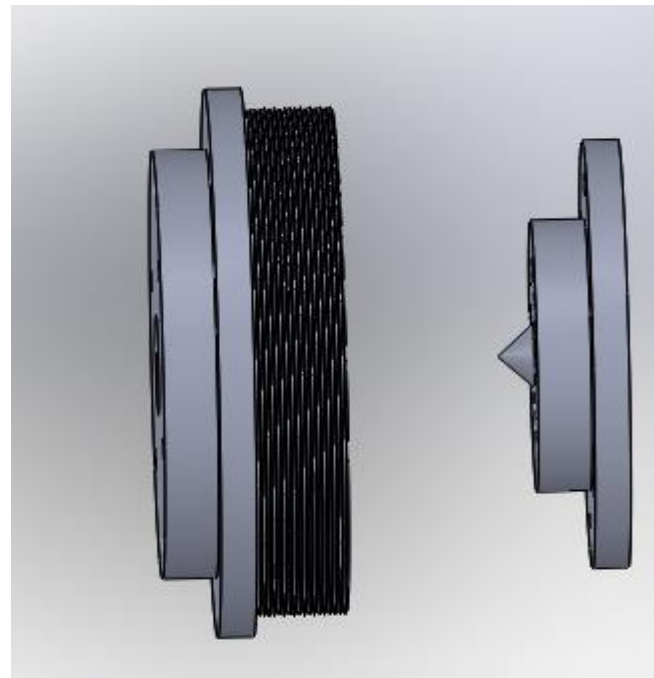


Figure 3-48 Injector Assembly

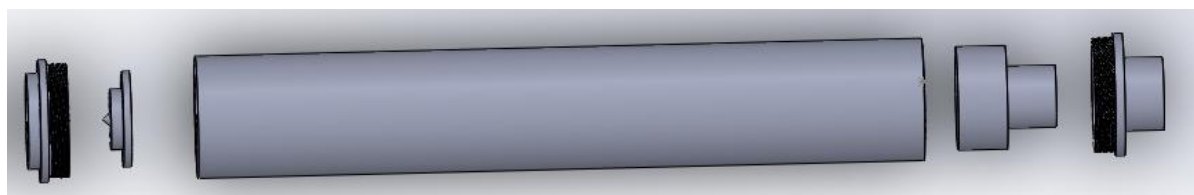


Figure 3-49 Rocket Assembly Exploded View

3.13 Analysis

3.13.1 Chamber

To ensure that the combustion chamber can bear the combustion pressure of 8 MPa, a finite element model was created to show major stress point on the chamber under load. The figure shows the chamber can withstand the applied pressure on the internal walls of the chamber with temperature conditions of 350 C. The FEA Model is tested using the solidworks file imported into Ansys Workbench. The material properties of Aluminium 6061-T6 were taken from ASM Material Data Sheet.

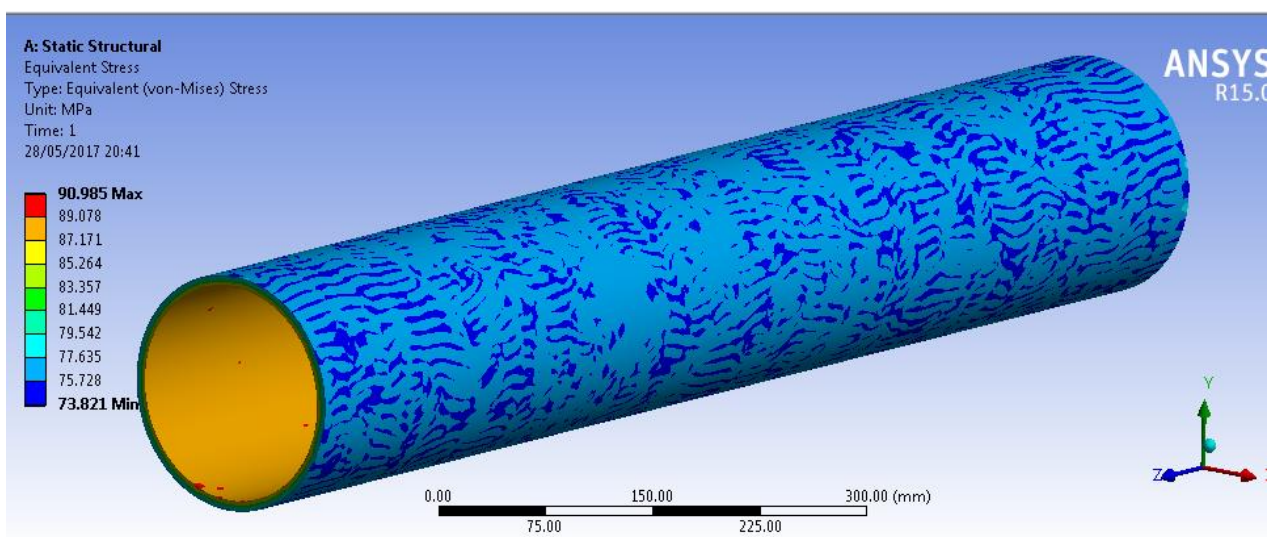


Figure 3-50: FEA simulations on the Combustion chamber

3.13.2 Injector Disc

Injector disk was the part which caused the oxidizer flow to swirl, keeping in mind that the injector would have to diverge ample amount of oxidizer flow coming at 1.3Kg/s. The oxidizer pressure would itself be at 80 Mpa causing stresses on the injector. The injector disk is to be constrained from 6 bolts which would hold the whole assembly together. FEA simulations were done check if the injector disk can bear the corresponding load. The simulations satisfied the design as the stresses induced were below the tensile yield strength. The material selected for the part was Alumunium 6061-T6.

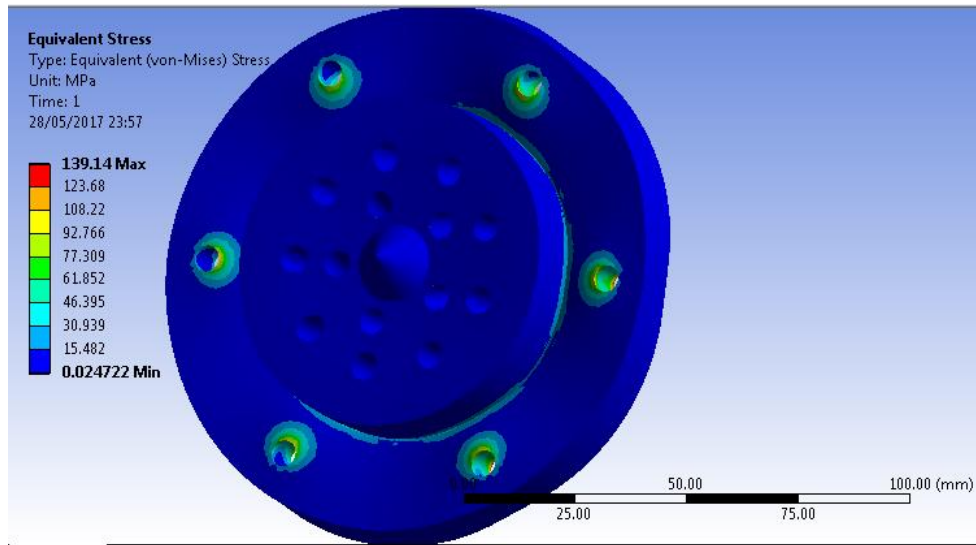


Figure 3-51 Injector Disc FEA Simulation (view 1)

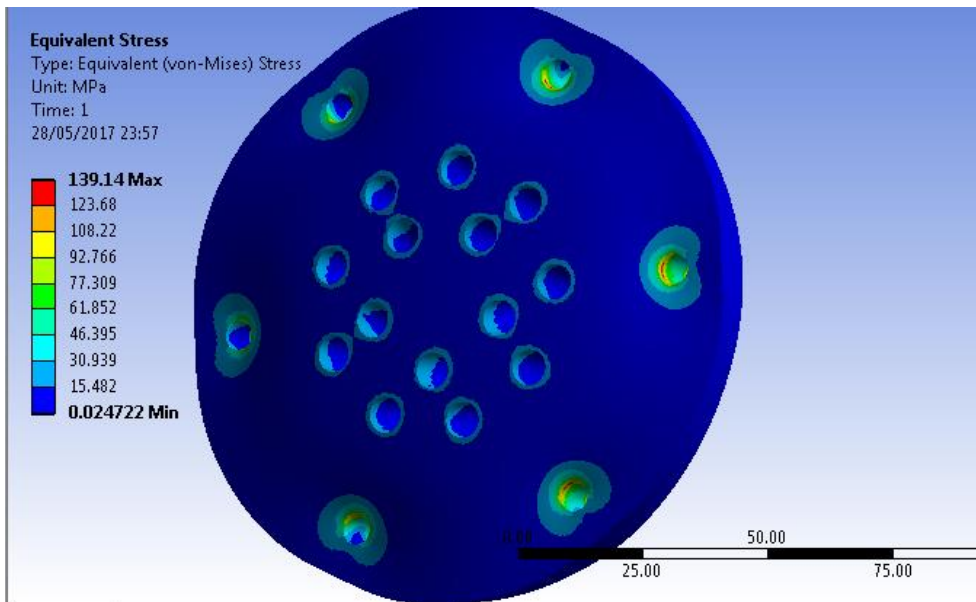


Figure 3-52 Injector Disc FEA Simulation (view 2)

3.13.3 Injector Cap

Injector cap is used to hold the front part of the assembly together and would be the first in line to bear the oxidizer pressure. Simulations on Ansys Workbench were conducted at a pressure of 8 MPa. Von mises stress simulations satisfied the modelled part as the Max stress induced was below the Yield strength.

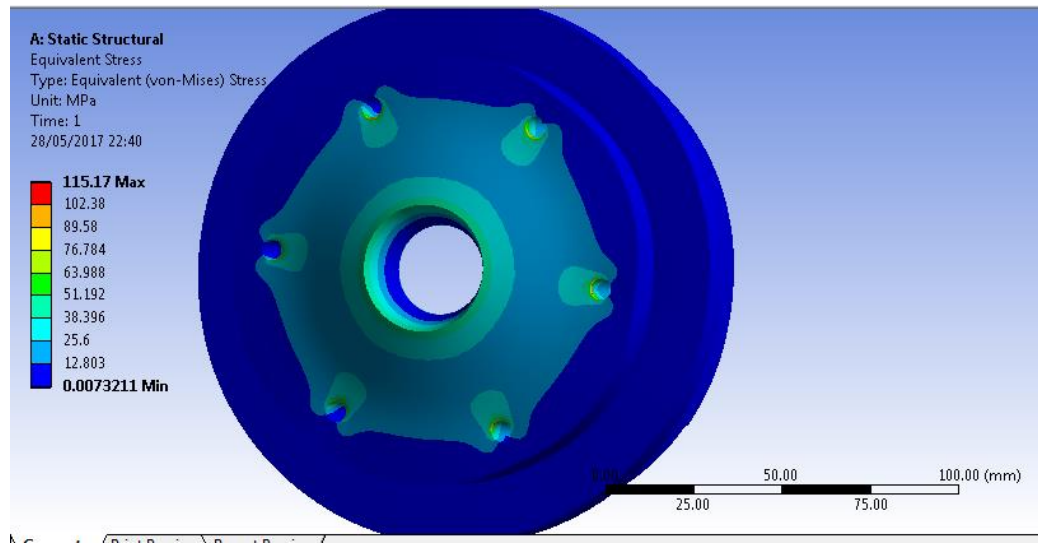


Figure 3-53 Injector Cap FEA Simulation (view 1)

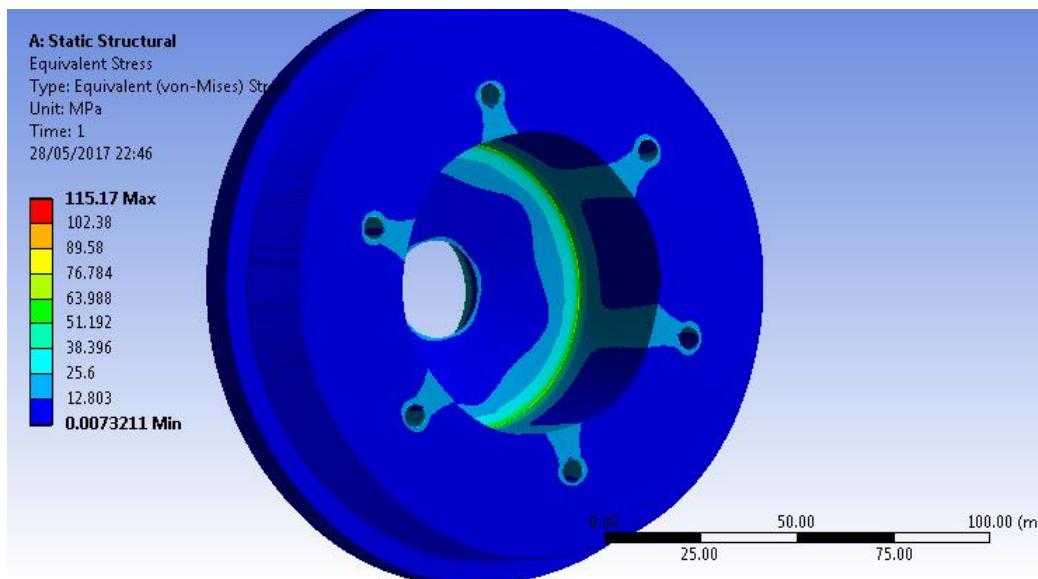


Figure 3-54 Injector Cap FEA Simulation (view 2)

3.13.4 Assembly

To ensure that the rocket assembly withstood the extreme pressure and the temperature conditions, the assembly of the rocket was simulated at the combustion pressure of 8Mpa. This analysis was conducted after introducing the fuel grain into the chamber. The wax's average thermal and mechanical properties were introduced according to its composition.

The simulations verified that the Von Mises stresses achieved were below the yield stress of the Aluminium 6061-T6. The regions having the most stress concentrations are the hole of the injector disc.

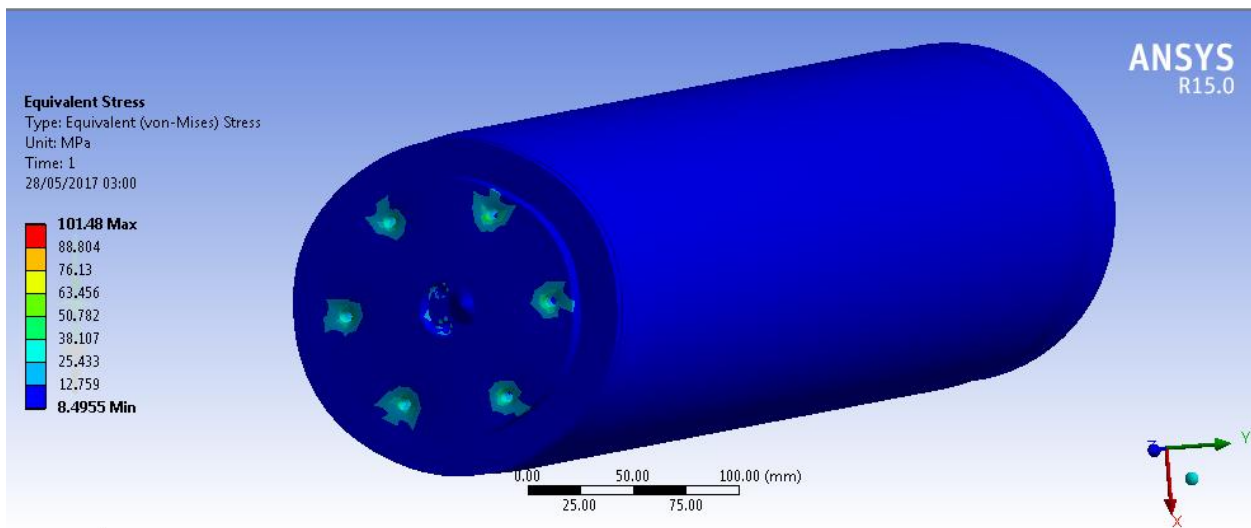


Figure 3-55 Assembly FEA Simulation

3.14 Flow Simulation

CFD was done with and without the fuel grain to verify if the choking conditions and the estimated exit velocity is achieved or not. To compensate the factor of increase in temperature, the oxidizer was given an initial temperature of 3500 Kelvins which is in accordance to the temperature of combustion calculated from the MATLAB code. Further to incorporate the effect of increase in mass flow because of combustion, the mass flow of oxidizer was further increased to 1.3 kg/s. Figures show the flow simulation of the oxidizer without the fuel grain.

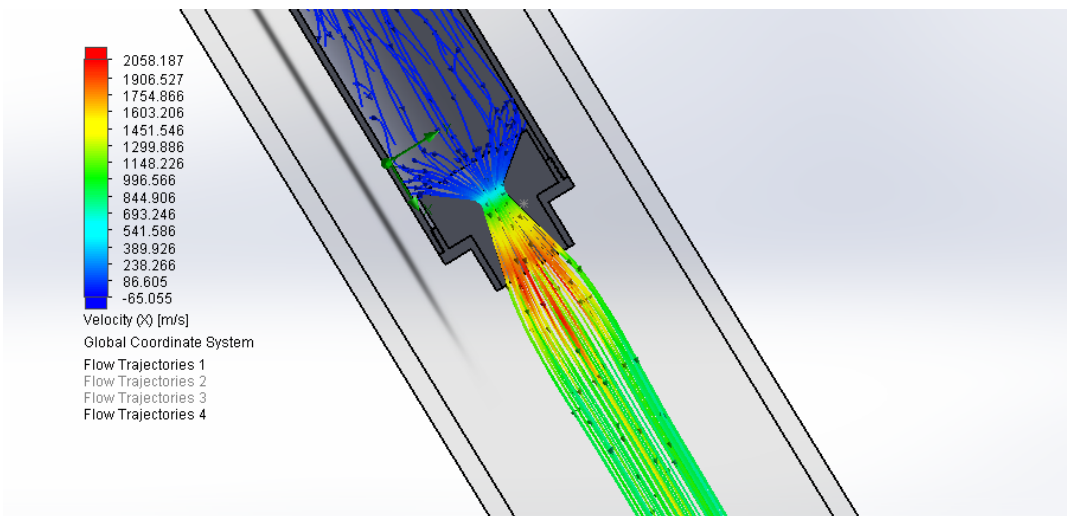


Figure 3-56 Velocity Simulation without Fuel Grain

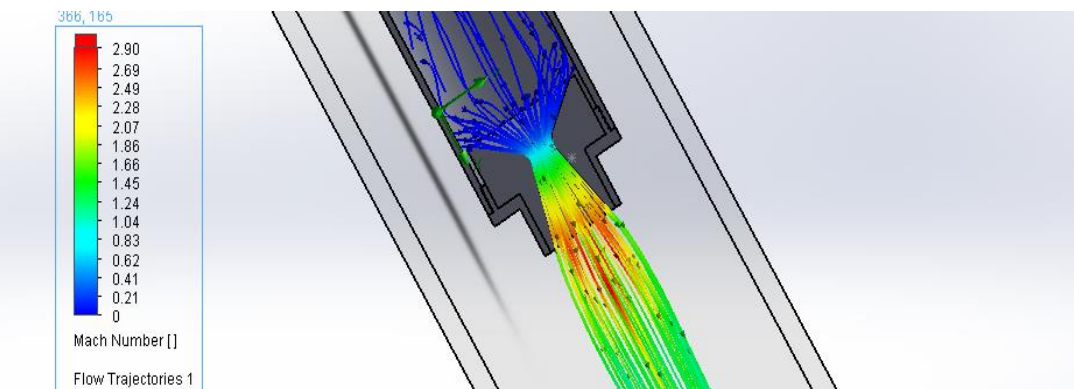


Figure 3-57 Mach No. Simulation without Fuel Grain

It can be observed in the above images that the Mach number at the throat is 1 and the exit velocity is approx. 2058 m/s.

The **Figures 3-57 and 3-58** show the CFD of the rocket engine with the fuel grain provided the initial conditions are same (i.e inlet mass flow is 1.3kg/s and the temperature is 3500 Kelvin).

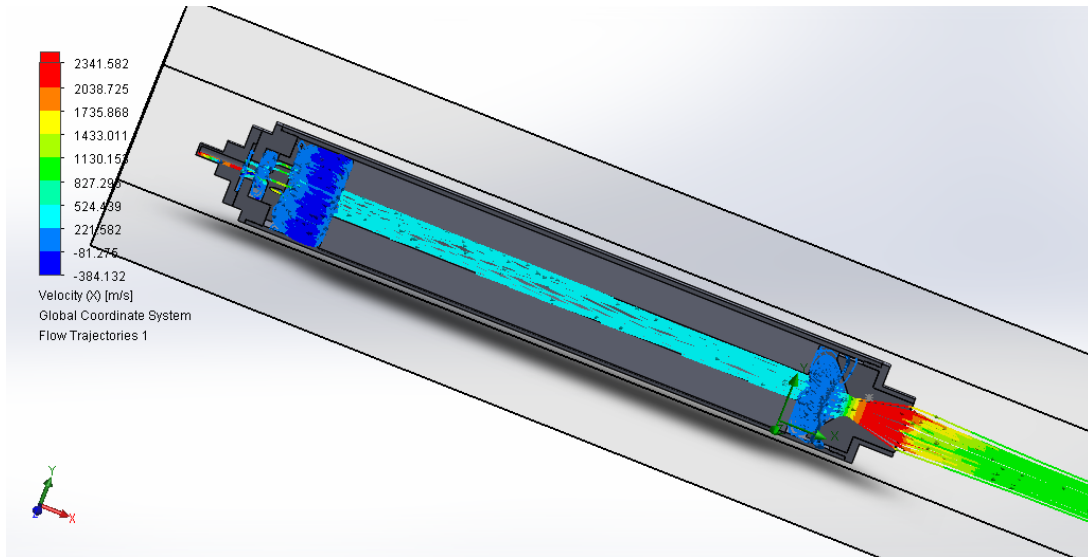


Figure 3-58 Velocity Simulation with Fuel Grain

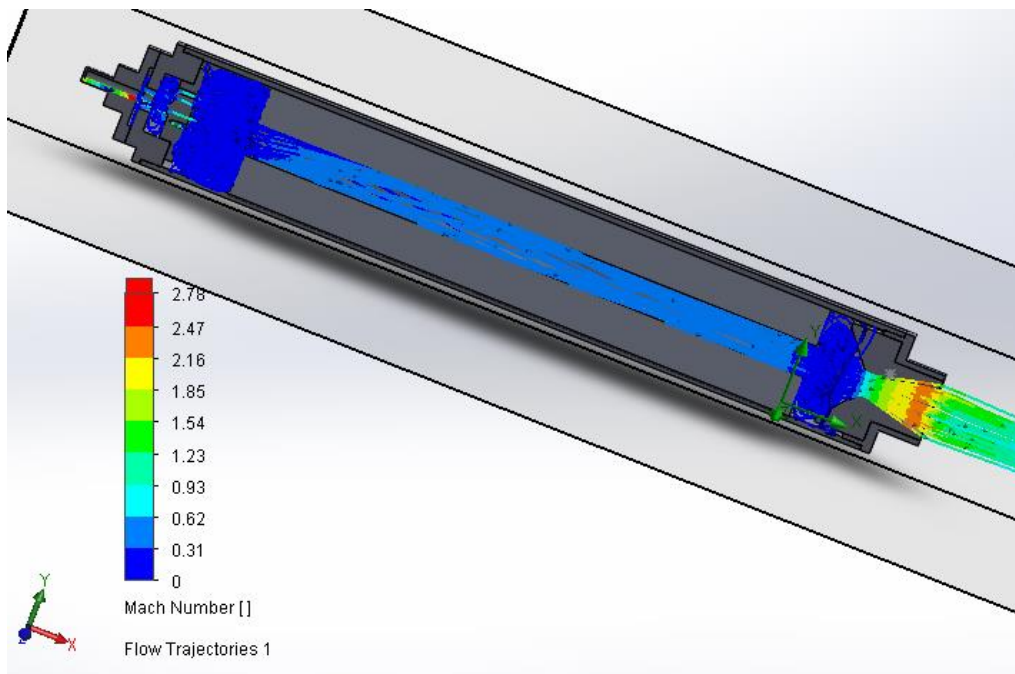


Figure 3-59 Mach No. Simulation with Fuel Grain

The Mach number is still choking but the velocity increases at the exit to 2300 m/s which is similar to the results obtained through calculations.

3.15 Test Rigs

The test rig was constructed with MS angle iron. It consisted of a railing on which the rocket was clamped and held safely in place. This allowed the rocket Engine to have only one degree of freedom which was against the load cell mounted on the test rig. This makes the linear displacement of the rocket directly create a moment on the load cell thus enables the load cell to measure the thrust. **Figures 3-59** shows the CAD diagrams of the test bench.

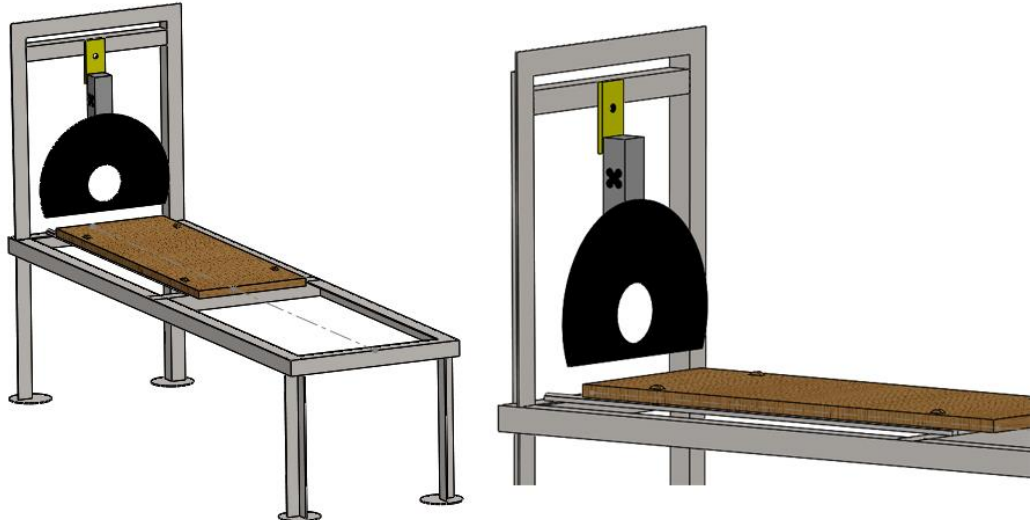


Figure 3-60 Test Rig CAD Drawings



Figure 3-61 Test Rig with Rocket Mounted



Figure 3-62 Load Cell

Chapter 4: Safety

It was made sure that all the tests, the molding process and all the other processes involved in the testing of the 5000 Newton Hybrid Rocket Engine were safe.

- During machining, it was made sure that the machinist was equipped with safety goggles and gloves.
- During the moulding, it was made sure that all the people handling the mould were wearing gloves and safety shoes to prevent burns. This was done in the DSU workshop which was equipped with firefighting equipment.
- During the testing, it was made sure that the rocket engine and the operator are at a safe distance of at least 30 ft. The rocket Engine was also kept in a pit (at a lower altitude) to make sure if it blows up, there should be minimum probability of any shrapnel hitting the operator or the people around. Fire extinguishers were placed nearby in case of fire.

Figure 4-1 shows the machinist equipped with goggles and gloves while grinding the mandrel.



Figure 4-1 Grinding with Safety

Figure 4-2 shows the handling of the mould with the use of gloves.



Figure 4-2 Mould Handling with Safety

Figure 4-3 shows the safe distance that was kept from the rocket and also that the rocket is placed at lower height.

Figure 4-3 Safe Distance



Chapter 5: Manufacturing Processes

Two solid cylindrical Aluminum 6061-T6 pieces were bought, along with a 940 mm long hollow pipe with thickness of 11mm and an internal dia of 136mm.

5.1 Combustion Chamber

Combustion chamber is an Aluminum 6061-T6 hollow cylinder that was subjected to threading using lathe machine operations. Care was taken during the manufacturing process as a well centered lathe along with steady rest was used to avoid the harmonics of the tube. Special care was given to the threads of the chamber as they could have caused fitting issues later. The length of the cylinder was kept 914mm. According to the designed Factor of Safety, the thickness of the cylinder should be 10mm at the inner diameter of 139.7mm.



The threads on the chamber were 16 tpi. All the other components had the same thread sizes.

5.2 Injector Assembly

The injector assembly was fabricated in two parts, the first part that was actually in contact with cylinder walls is called the ‘Injector Base’ and the other part which caused swirl motion of the oxidizer was called the ‘Injector Disc’. Both the parts were assembled with each other using Allen bolts. The machining processes involved in this part were stepping, threading, tapering, turning, and drilling. The machines required to fabricate these parts were Lathe Machine and Drill Press.

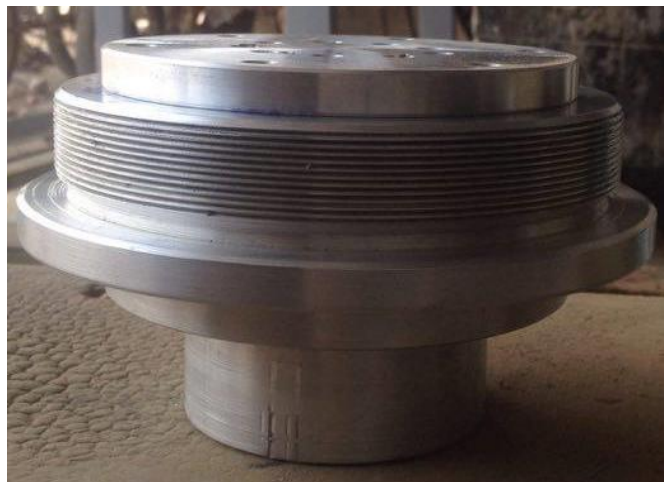


Figure 5-1 Injector assembly

5.2.1 Injector Base

Injector base consisted of threads that were used to fit it into the combustion chamber, the oxidizer inlet had to be threaded as the nozzle which was directly crimped with pipes had to fit in through these threads. The Injector connected the oxidizer pipes and the rocket. **Figure 5-1** shows the injector cap assembled with disc.



Figure 5-2: Injector assembled in the rocket (pipes are shown too)



Figure 5-3 Injector cap isometric View



Figure 5-4 Injector cap Top View

5.2.2 Injector disc

The injector disc consisted of a divergent cone which was used to diverge the oxidizer flow towards the hole. It consists of 9 holes of diameter 6 mm at a PCD of 50mm and 5 holes of diameter 6mm at a PCD of 29.14mm. The 5 holes are at an angle of 20 degrees from the vertical axis. The angular holes were drilled by making a wooden jig with a slope of 20 degree. Stepping, facing, taper turning and drilling were processes required to manufacture these parts.

The step contains 6 thru-holes which are used to assemble the injector disc and injector base together via Allen bolts and nuts.



Figure 5-5 Injector Disc Top View



Figure 5-6 Injector Disc Isometric View

5.3 Con-Di

The con-di nozzle was made of graphite. The operations used in this part were stepping, taper turning and parting. The diameter of the throat was kept at a convergent angle of 52 degrees whereas the divergent angle was kept at 14 degrees. The throat diameter was kept at 23mm.



Figure 5-7 Con-Di Isometric View

5.4 End cap

End cap was made of Aluminum 6061-T6. It has threads and a bore in which the Con-Di rests and threads are used to assemble it with the combustion chamber.



Figure 5-8 Manufacturing of End Cap



Figure 5-9 End Cap Isometric View

Chapter 6: Results and Conclusion

6.1 Results and discussion

Post-fire test analysis were conducted on the rocket and the test bench. Unfortunately during the test, the load bearing plate was permanently deformed due to the Thrust. However, uniform flame geometry was achieved with a burn time of 6 seconds. The operator intentionally shut off rocket because acoustics level went too high.

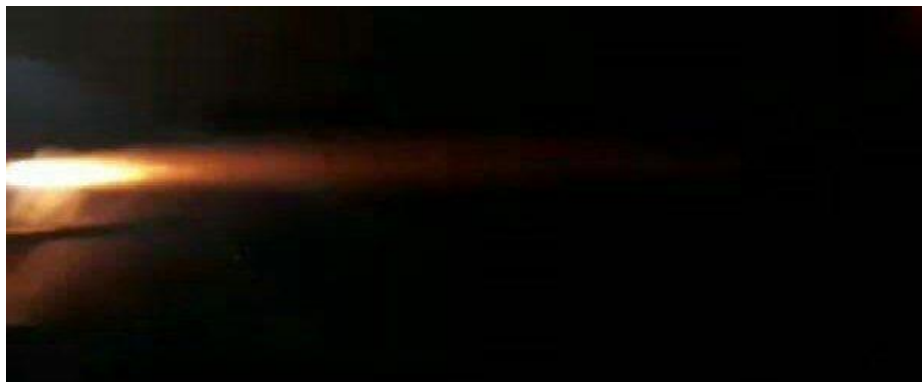


Figure 6-1 Flame Geometry 1



Figure 6-2 Flame Geometry 2

Unfortunately during the test, the camera tripod fell off due to soft ground because of which only limited amount of visual evidence was captured.

The permanent deformation in the load cell assembly affected the results and because of which the thrust curve couldn't be attained. The deformation in the load cell caused by the impact force resulted in malfunction of load cell.

The Images below show the bending in the MS supporting part caused due to the extreme loads. The Semi circular plate acted as a cantilever and caused the supporting plate to distort permanently. Some welds between the supporting part and the test bench were also cracked. Distortion in the hole of supporting plate was also observed.



Figure 6-3 MS Plate



Figure 6-4 Mild Steel Plate with Broken Welds (post test)



Figure 6-5 Mild Steel Plate Front View (post test)

Failure analysis was then conducted on ANSYS Workbench to simulate the whole test. In order verify if considerable amount thrust was actually achieved or not, SOLIDWORKS model of the test bench was imported in the ANSYS Workbench. 5000N of force was applied on the semicircular plate, while the the test bench was constrained from the base.

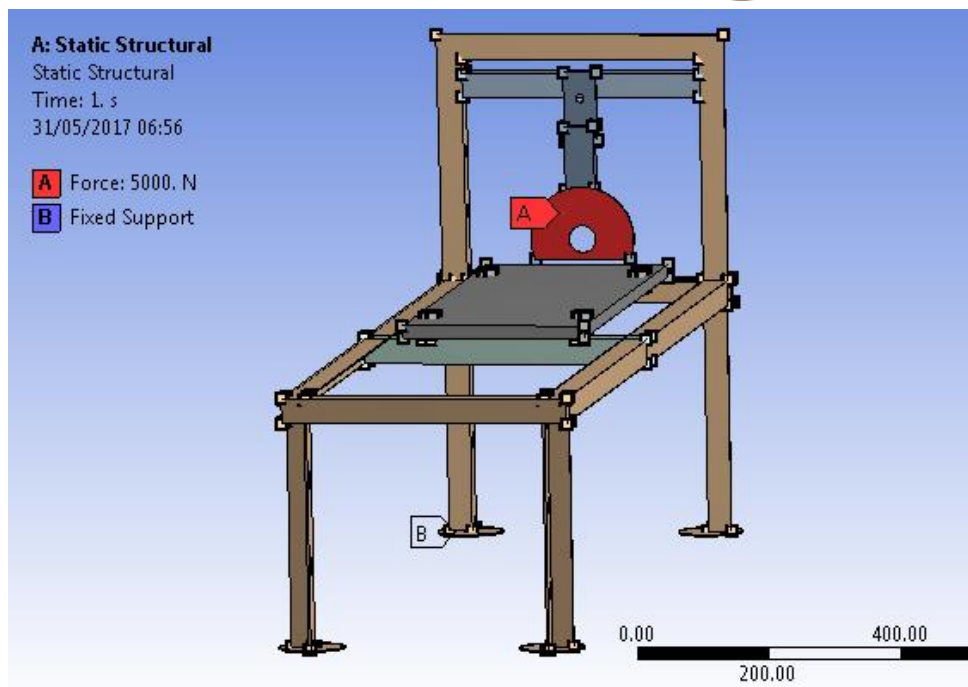


Figure 6-6 Test Rig Failure Analysis 1

The simulations showed similar deflection in the load cell assembly and a max deflection of about 21mm in the direction of the force.

Stress concentrations occur in the region of the hole and the weld joints similar to the actual results shown in Figure 6-5.

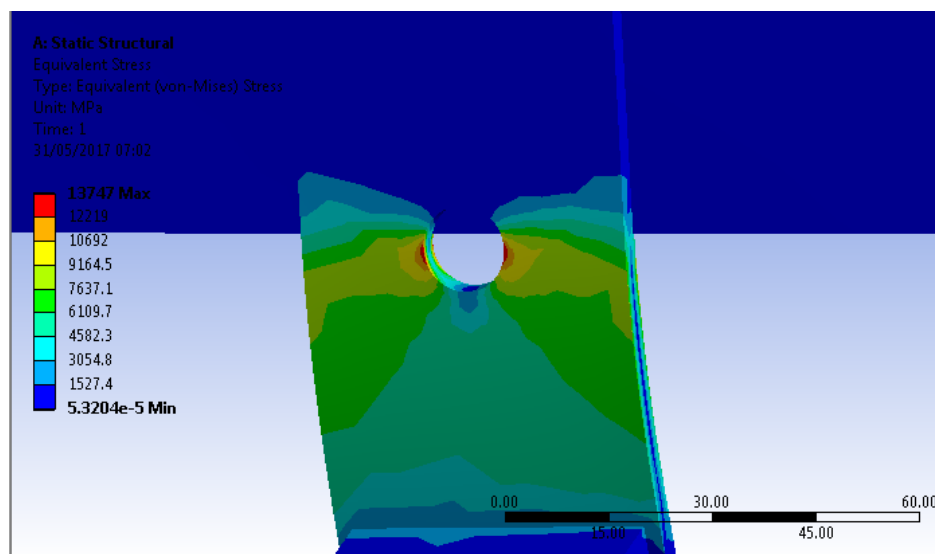


Figure 6-7 Test Rig Failure Analysis 2

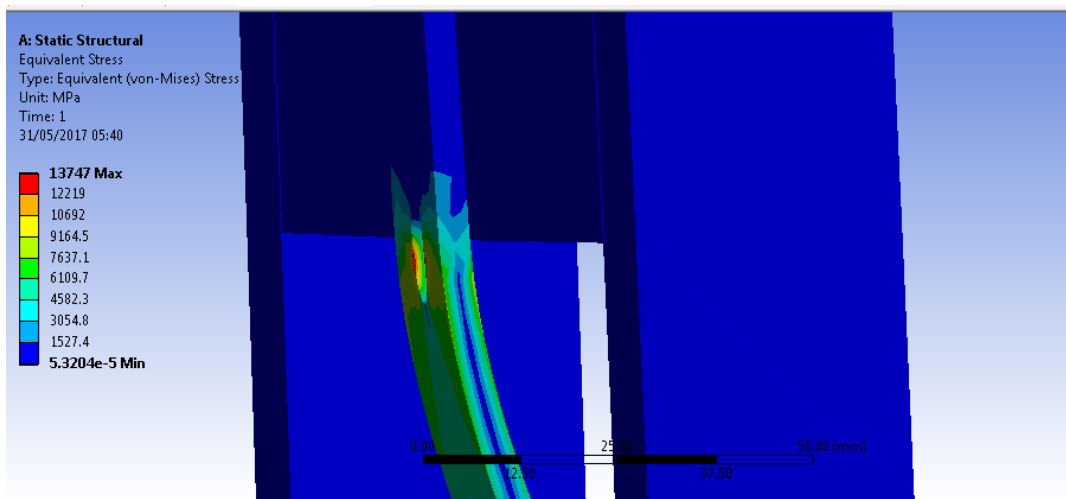


Figure 6-8 Test Rig Failure Analysis 3

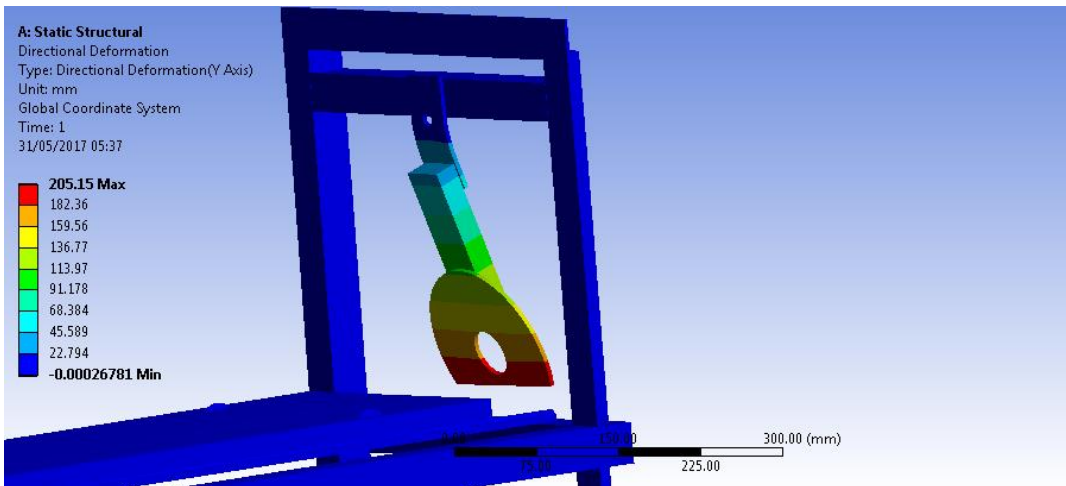


Figure 6-9 Test Rig Failure Analysis 4

The simulations results for the failure of test bench were very similar to the acutal results, which closely verified the fact that a good amount of thrust was acheived.

In order to further compare the results, the actual deflection of the plate was measured using Engineering Drawing skills (**Figure 6-11**). The actual maximum deflection at the semicircular plate end came out to be approx. 17.4mm as compared to the 21mm achieved from simulations.

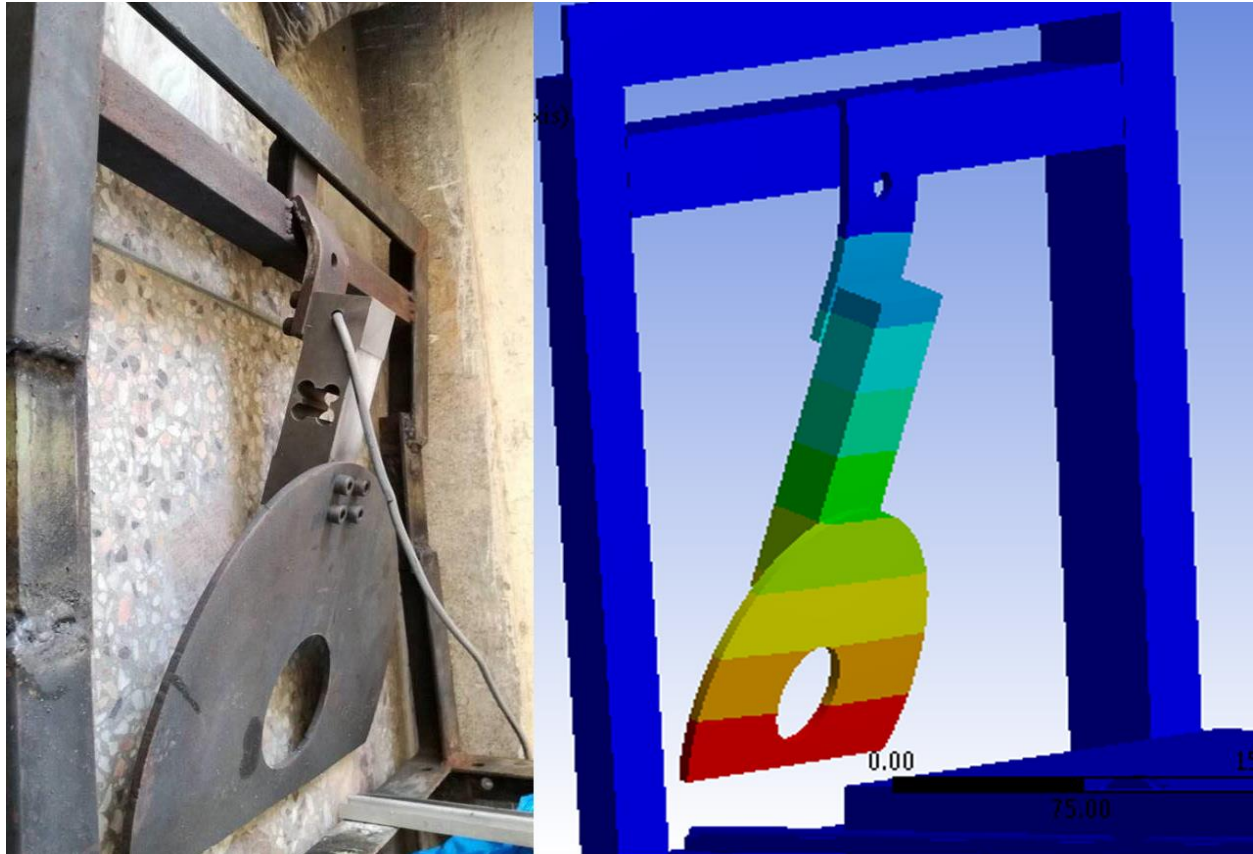


Figure 6-10 Test Rig Failure Analysis 5

The **Figure 6-10** shows the similarity of the simulations and the real life test conducted.

The simulations also suggest severe stress concentration at the supporting plate's hole and at the region of welds between the supporting plate and test bench, which were actually observed to be distorted and cracked respectively in the test bench.

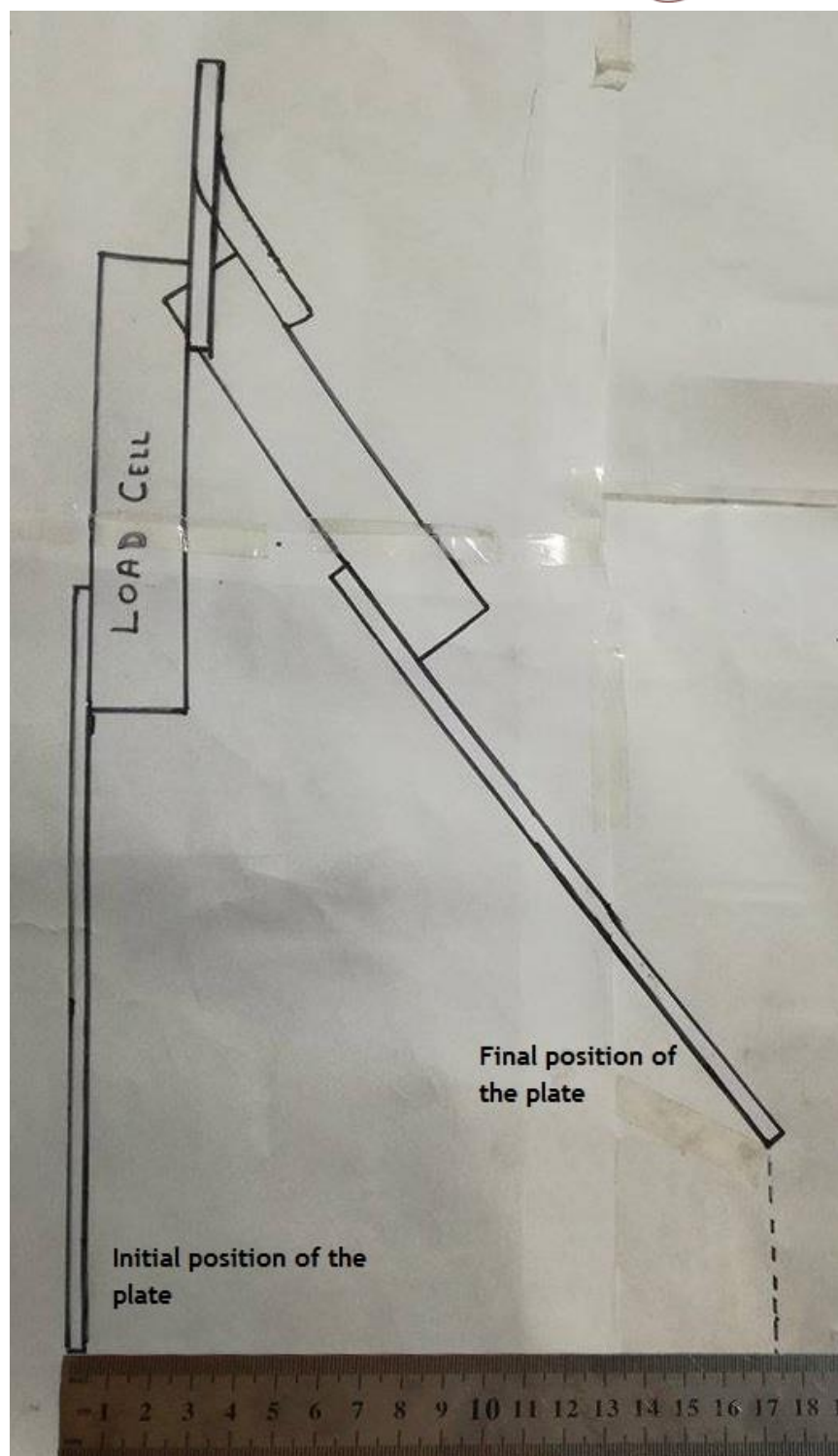


Figure 6-11 Manual Deflection Measurement

6.2 Conclusion

6.2.1 Objectives acheived

All the Objectives present in the SOR termed as the primary goals of the project are achieved the accomplishments include

- It was made sure to check that the rocket engine is whether restart able or not , in order to ensure this the operator had to close the oxidizer valve/regulator and has to open it again we tested it form an interval of 10 secs and it restarted.
- The designing, simulations and the manufacturing of the rocket engine is done.
- Test scale rocket engines were designed and manufacture the composition of the fuel was tested on these small scale engines.
- The testing of different combinations of fuels are done , these tests were compared on the basis of regression rates
- The static thrust test stand was designed and manufactured, Load cell was used to measure the thrust.
- The fuel composition was optimized on the basis of regression rates
- Swirl flow injector was designed, manufactured and tested.
- The Nozzle was made of Graphite, which is thermally stable and can withstand high temperatures.
- We can not actually test and fire the Rocket engine because of HES issues and security issues however it can be easily tested in a flight by properly making a contraption to keep both oxidizer tanks and the rocket engine itself.

6.2.2 Accomplishments:

- We have received acknowledgment from Express Tribune at our work on the Hybrid Rocket Engines
<https://tribune.com.pk/story/1170610/lift-off-pakistans-first-ever-hybrid-rocket-readying-launch/>
- We have won the best project award at the World Space Fair held by Space and Upper Atmosphere Research Commission (SUPARCO).
<http://nationalcourier.pk/metropolis/debutant-dsu-secures-1st-2nd-positions-space-fair/>
- Submitted a research paper at researchgate and took part in DICE automotive
<https://www.researchgate.net/project/Hybrid-rocket-propulsion>

Multiple tests were conducted on the lab scale models

- <https://www.youtube.com/watch?v=fw5zEtmObws>
- <https://www.youtube.com/watch?v=d8kBpVOVBkE>
- <https://www.youtube.com/watch?v=gKFORbNn8gU>

References

- https://www.researchgate.net/publication/290095691_Microcrystalline_paraffin_wax_as_fuel_for_Hybrid_Rocket_Engine
- ‘Recent Advances In Hybrid Propulsion’ (B. Cantwell, A. Karabeyoglu and D. Altman, 2010)
- ‘Overview on hybrid propulsion’ (M. Calabro, 2011)
- ‘Status update report for the Peregrine Sounding Rocket Project: Part III’ (E. Doran, J. Dyer, M. Marzona, A. Karabeyoglu, G. Zilliac, R. Mosher, and B. Cantwell, 2009)
- Sutton, G.P. and Biblarz, O., “Rocket Propulsion Elements”, John Wiley and Sons, 7th Ed., MA, 2001.
- M. A. Karabeyoglu, Greg Zilliac, Brian J. Cantwell, Shane DeZilwaand Paul Castellucci, “Scale-up Tests of High Regression Rate Paraffin-Based Hybrid Rocket Fuels”, Journal of Propulsion and Power, Vol. 20, No. 6, p. 1037-1045, 2004.
- Elizabeth T. Jens, Ashley A. Chandler, Brian Cantwell, G Scott Hubbard, and Flora Mechentel. "Combustion Visualization of Paraffin-Based Hybrid Rocket Fuel at Elevated Pressures", 50th AIAA/ASME/SAE/ASEE Joint Propulsion Conference, Propulsion and Energy Forum, 2014.
- Alessandro Mazzetti, Laura Merotto, and Giordano Pinarello, “Paraffin-based hybrid rocket engines applications: A review and a market perspective,” ActaAstronautica, 2016.
- “Modern engineering for Design of Liquid Propellant Rocket Engines” by Diexter K.Huzel and David H.Huang
- Bilal A. Siddiqui, K. Siddiqui, W. Aslam, U. Shakeel, and S. M. A. Shah, “Design, Build, Fire: Pakistan's First Hybrid Rocket Engine and University Run Rocketry Program”, 5th International Conference on Aerospace Science and Engineering (ICASE 2017) November 14 - 16, 2017 Institute of Space Technology, Islamabad, Pakistan.

- Lee, Tsong-Sheng, and A. Potapkin. The Performance of a Hybrid Rocket with Swirl GOx Injection. Novosibirsk, Russia: Institute of Theoretical and Applied Mechanics Institutskaya, 2002.
- Huzel, Dieter K., and David H. Huang. Modern Engineering For Design of Liquid Propellant Rocket Engines. Washington D.C.: American Institute of Aeronautics and Astronautics, 1992
- Munson, Bruce R., Donald F. Young, and Theodore H. Okiishi. Fundamentals of Fluid Mechanics. 5th ed. Wiley, 2005.

Appendix

Appendix A

Design, Build, Fire: Pakistan's First Hybrid Rocket Engine and University Run Rocketry Program

B.A. Siddiqui¹, K. Siddiqui¹, W. Aslam¹, U. Shakeel¹ and S.M.A. Shah¹

DHA Suffa University, Karachi, Pakistan ¹

B.A. Siddiqui (airbilal@dsu.edu.pk) ¹

Abstract

Hybrid rocket engine technology is a clean form of rocket propulsion which has no toxic exhaust. It uses solid fuel (paraffin, HTPB etc.) and liquid or gaseous oxidizer (oxygen, N₂O₂ etc.), so that the product is water (steam) and carbon dioxide. Over the last two decades, this technology has revolutionized the space industry and is now being considered for space launch. Over the course of the last year, researchers at DHA Suffa University have developed hybrid rockets, the first (and only) of its kind program in Pakistan and only the third in Asia. This work describes the design and development of the first hybrid rocket engine as well its static and dynamic tests. The design is carried out on an in-house developed hybrid rocket design software implemented in MATLAB integrated with NASA's CEA software for thermochemical predictions. The static test rig is equipped with load cells and pressure sensors, while the dynamic test rig consists of a purpose built unmanned car equipped with inertial measurement unit and GPS sensors. The test is completely automated and wirelessly triggered. Data is logged using National Instruments MyRio board. Various fuel combinations have been tested on smaller "fuel qualifier" rockets, while prototypes have been build and tested from 4 to 12 inch diameters. Nozzle inserts are made of graphite while aluminum is used for all other parts. This work is an attempt to make hybrid rocket technology available to universities in the country as a cheap, clean and safe technology for implementing rocketry programs at the undergraduate and graduate levels.

Keywords: rocket; propulsion; paraffin wax; hybrid rocket engine; MATLAB